High Spin States in Nuclei:
Exotic Quantal Rotation
II

Umesh Garg

University of Notre Dame

Supported in part by the National Science Foundation

CNSSS17

August 23-29, 2017

"standard" γ-ray spectroscopic measurements:

- γ–γ coincidences → level structure
- Angular Distributions/Correlations
  → angular momentum transfer Δ*L*
- Linear Polarizations → parity
- Lifetimes → transition probabilities

E*ΔL:* Electric, $\pi = (-1)^{\Delta L}$; E*2*

M*ΔL:* Magnetic, $\pi = (-1)^{\Delta L+1}$; M*1*

B(E2) → Q, β

animation courtesy of J. T. Matta

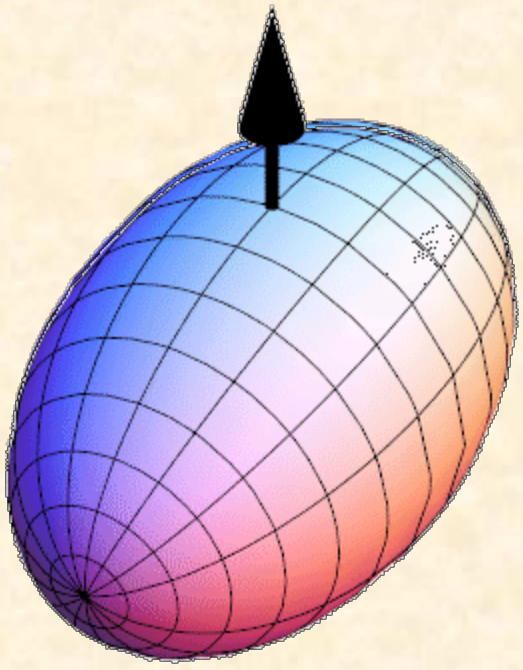

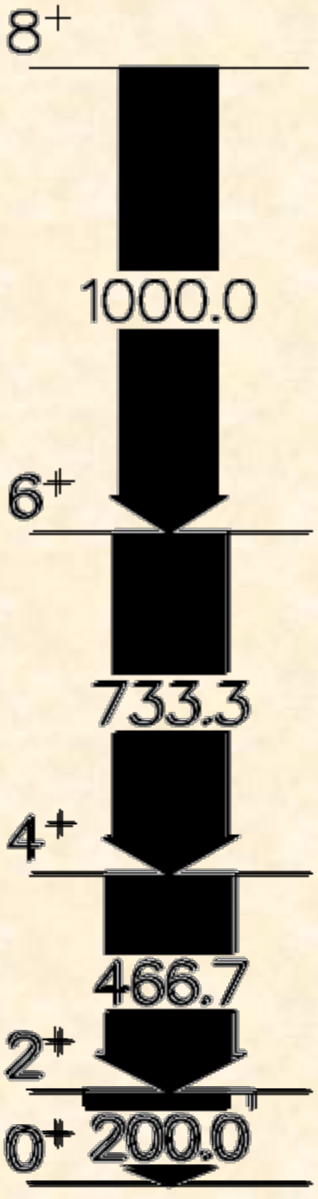

E2 transitions

$E_I = (\hbar^2/2\mathcal{J})\, I(I+1)$; $E\gamma = [\,](4I - 2)$

$\Delta E\gamma$ = Constant → "picket fence"

animation courtesy of J. T. Matta

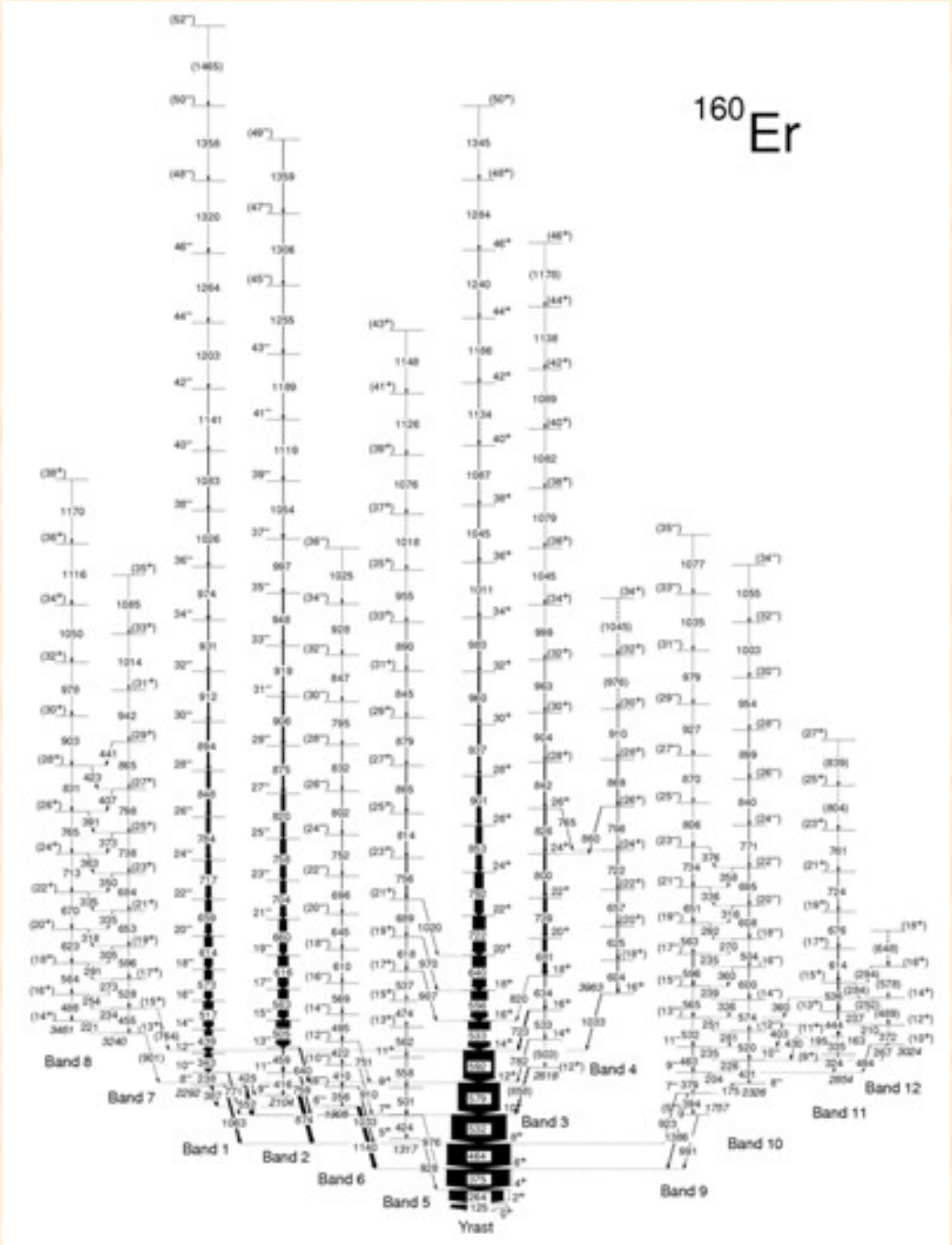
160Er
Band 1
Band 2
Band 3
Band 4
Band 5
Band 6
Band 7
Band 8
Band 9
Band 10
Band 11
Band 12
Yrast

Magnetic and Anti-Magnetic Rotation

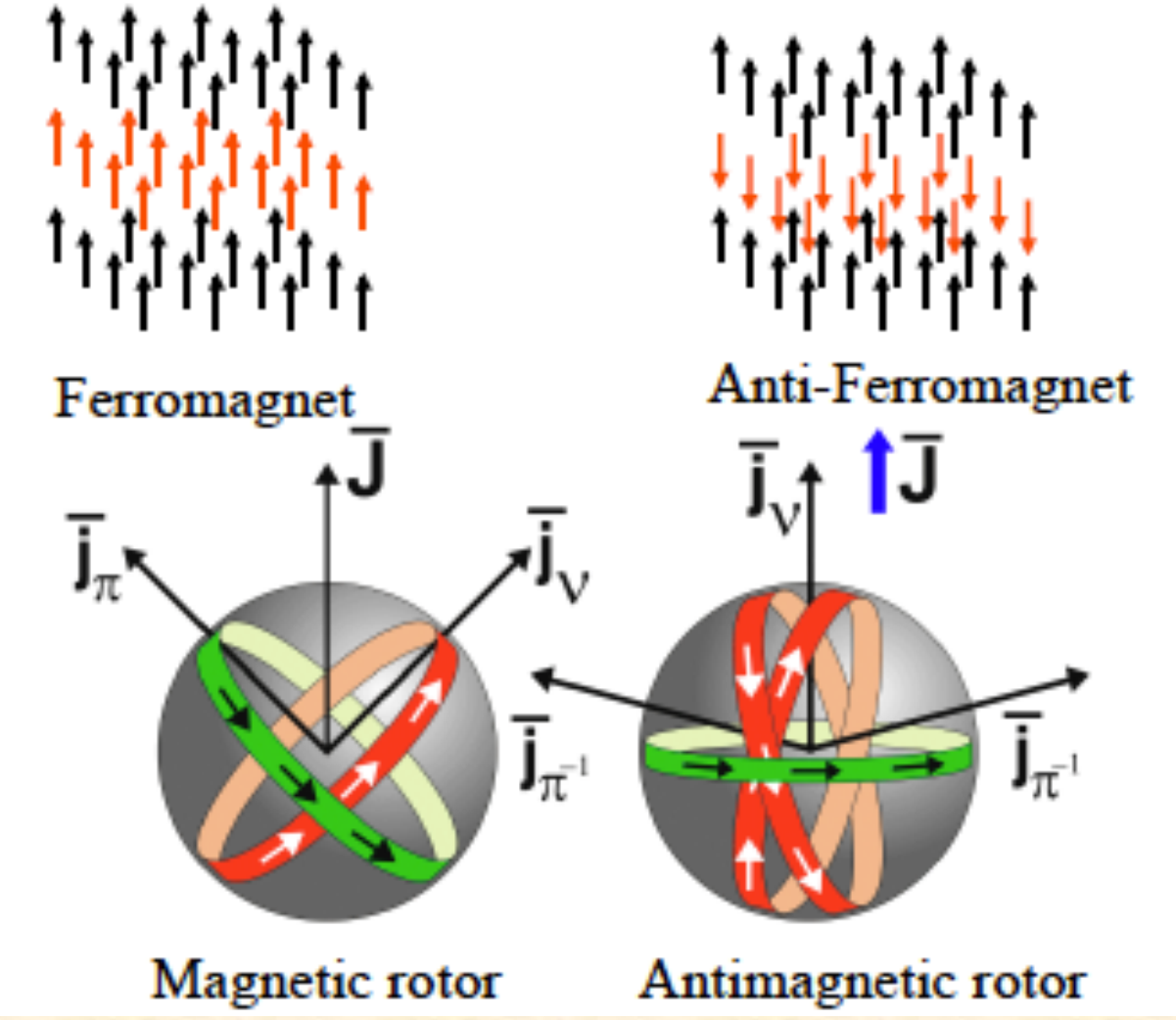

picture courtesy of S. Frauendorf

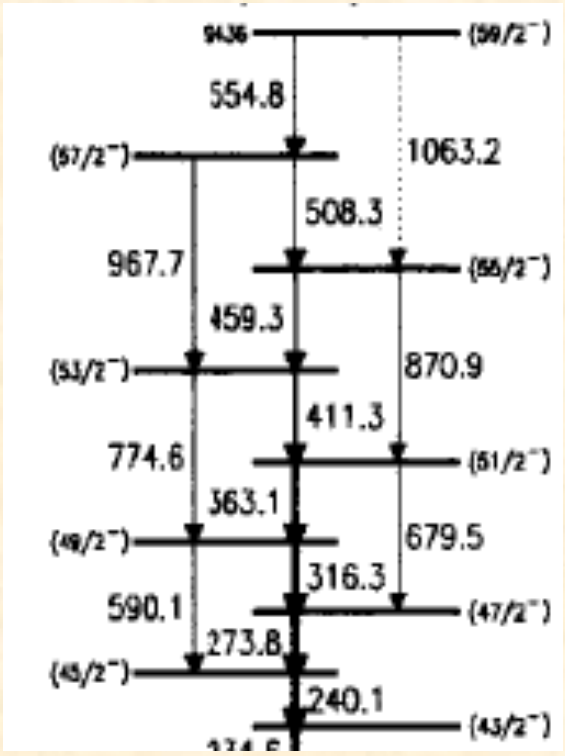

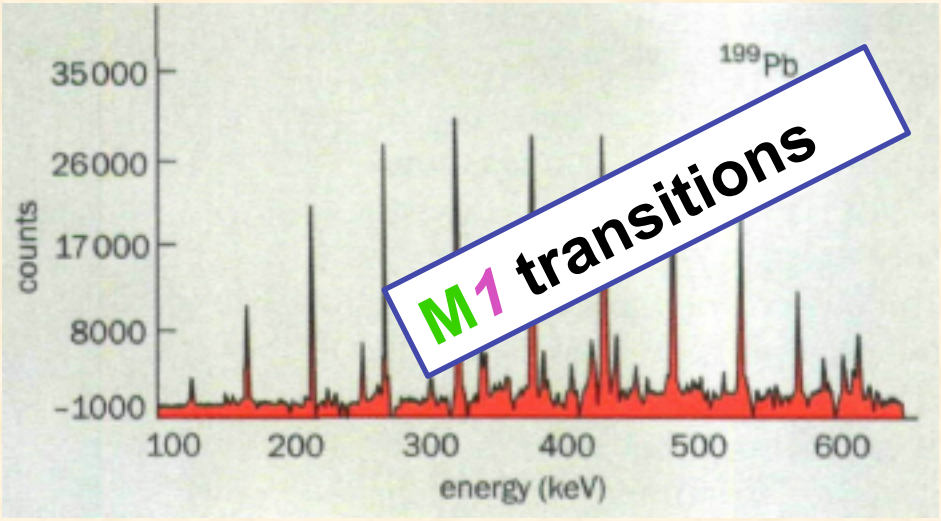

G. Baldsiefen *et al.*, Nucl. Phys. A **574**, 521 (1994).

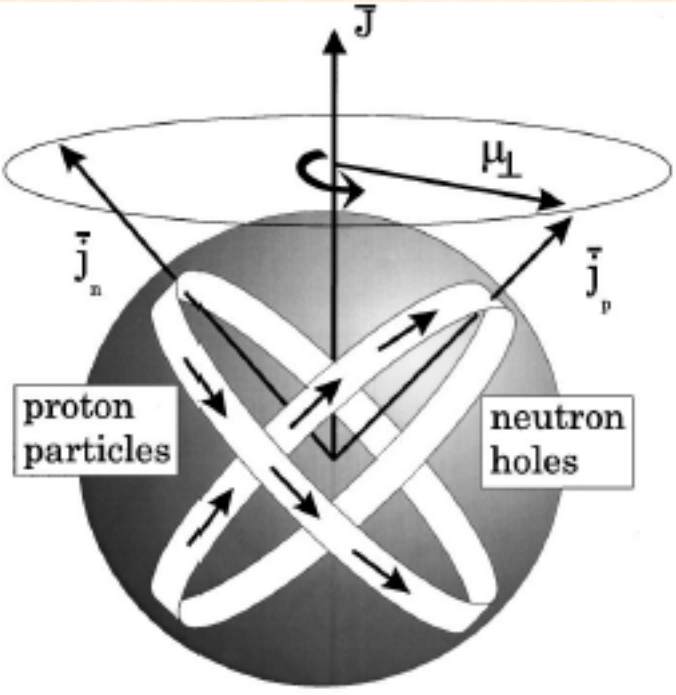

FIG. 18. Magnetic rotation. The high-j proton particles and neutron holes form current loops embedded in the near spherical mass distribution of the nucleus. These current loops as well as the associated transverse magnetic moment $\mu_\perp$ allow us to specify the angle ψ of rotation around the axis $\vec{J}$. The total angular momentum J increases by the gradual alignment of the particle and hole angular momenta $\vec{j}_p$ and $\vec{j}_n$. This is called the shears mechanism. The interaction due to shape polarization tries to keep $\vec{j}_p$ and $\vec{j}_n$ at a right angle, like the spring of a pair of shears. From Clark and Wadsworth, 1998.

S. Frauendorf, Rev. Mod. Phys. **73**, 463 (2001)

Tilted-axis Cranking

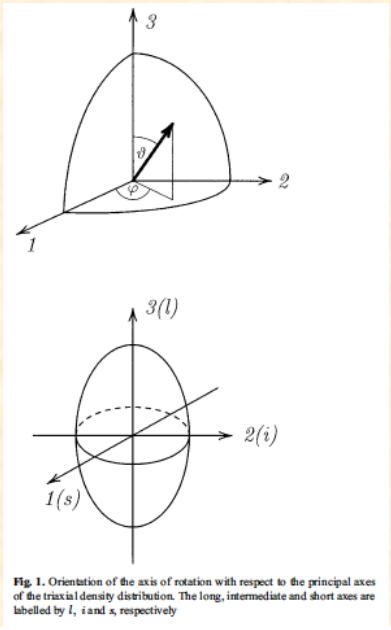

Fig. 1. Orientation of the axis of rotation with respect to the principal axes of the triaxial density distribution. The long, intermediate and short axes are labelled by l, i and s, respectively

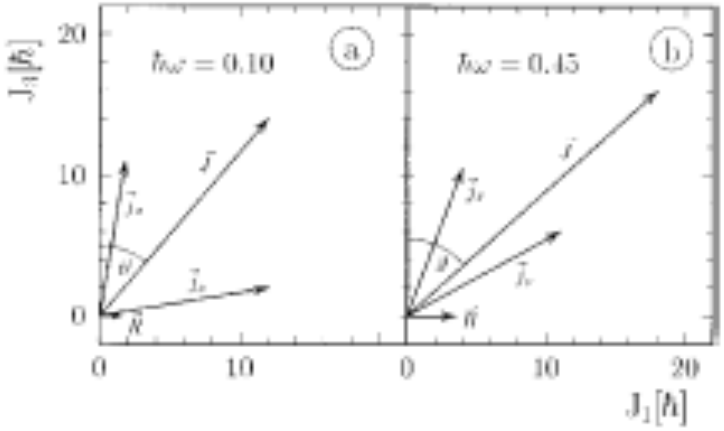

Fig. 2. Angular momentum composition of the shears bands with the high-j configuration $\pi h_{9/2}, \pi i_{13/2}, \pi s_{1/2}^{-2}, \nu i_{13/2}^{-2}$. Band 2 in ^{199}Pb (cf. [6]) has this configuration combined with a quasineutron on a low-j-fp orbital

S. Frauendorf, Z Phys. A **358**, 163 (1997)

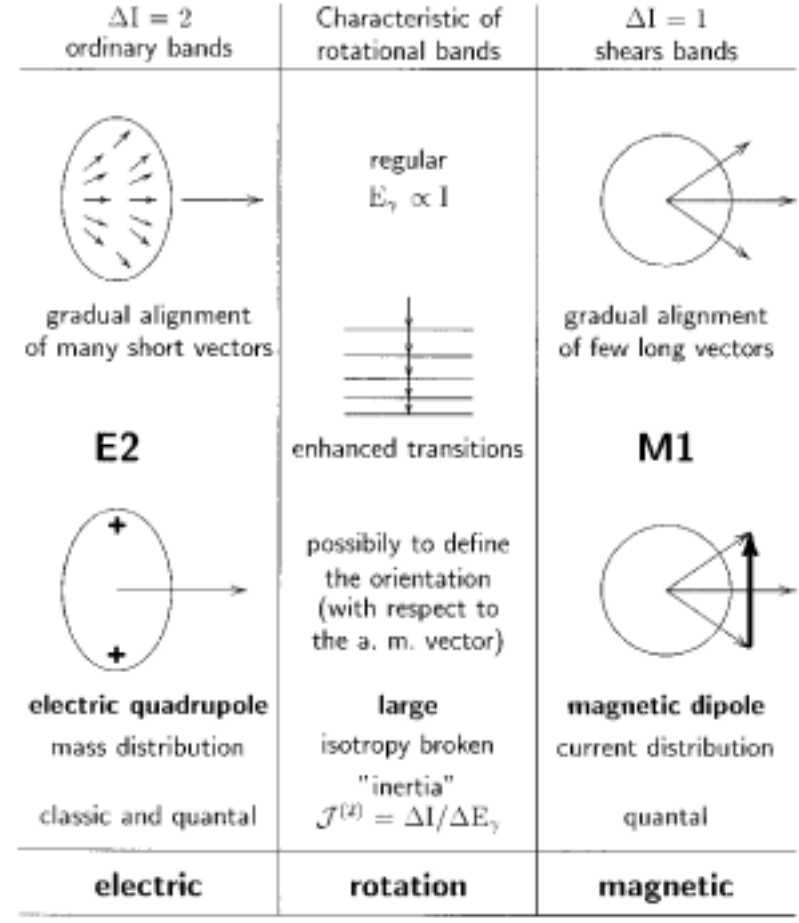

Fig. 4. The relation between electric and magnetic rotation

Moments of Inertia, $\mathcal{J}^{(2)}$, are substantial ~20 MeV^{-1}
B(M1) values are very large (several μ_N^2)
and decrease with spin.
Very small B(E2)s for crossover transitions (β <0.1)
$\mathcal{J}^{(2)}$/B(E2) very large
(>100 MeV^{-1}(eb)$^{-2}$, compared with ~10 for "normal")

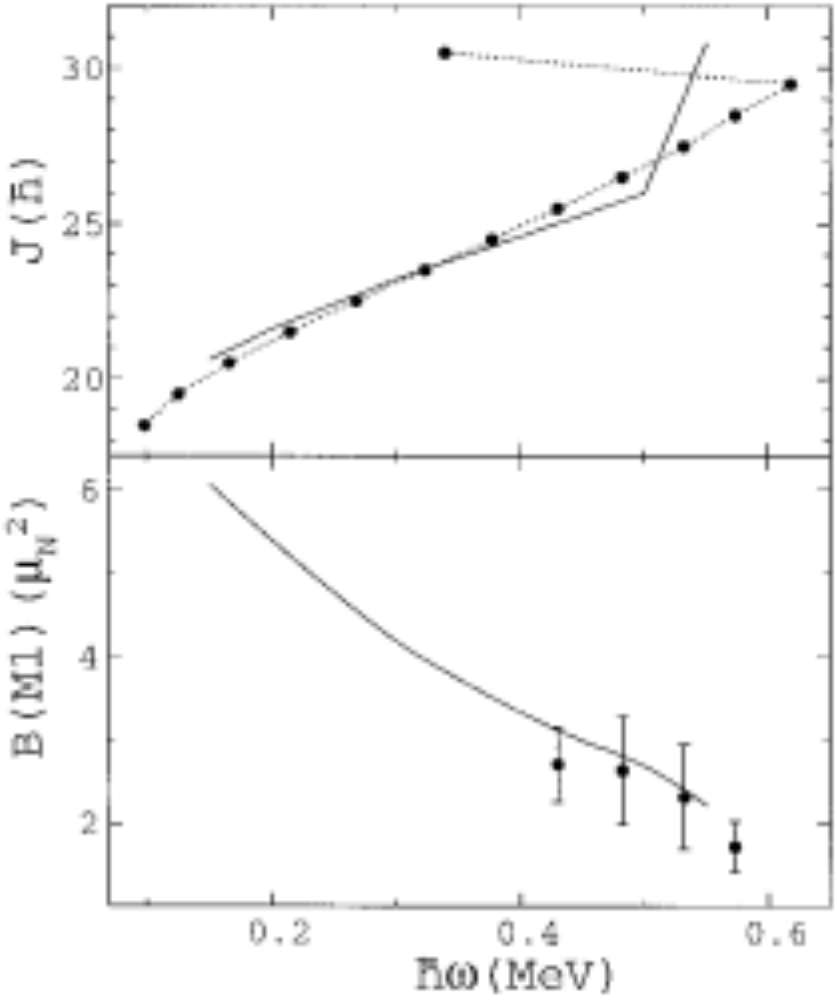

Fig. 3. Angular momentum and $BM1$ values as functions of the rotational frequency for band 2 in ^{199}Pb. For the configuration cf. Fig 2. *Full lines* are the TAC calculation. Points are the experimental data from [6, 8, 9]. In (3) the experimental value of 0.5 is taken for the spin attenuation factor of the $i_{13/2}$ neutrons

S. Frauendorf, Z Phys. A **358**, 163 (1997)

Anti-Magnetic Rotation

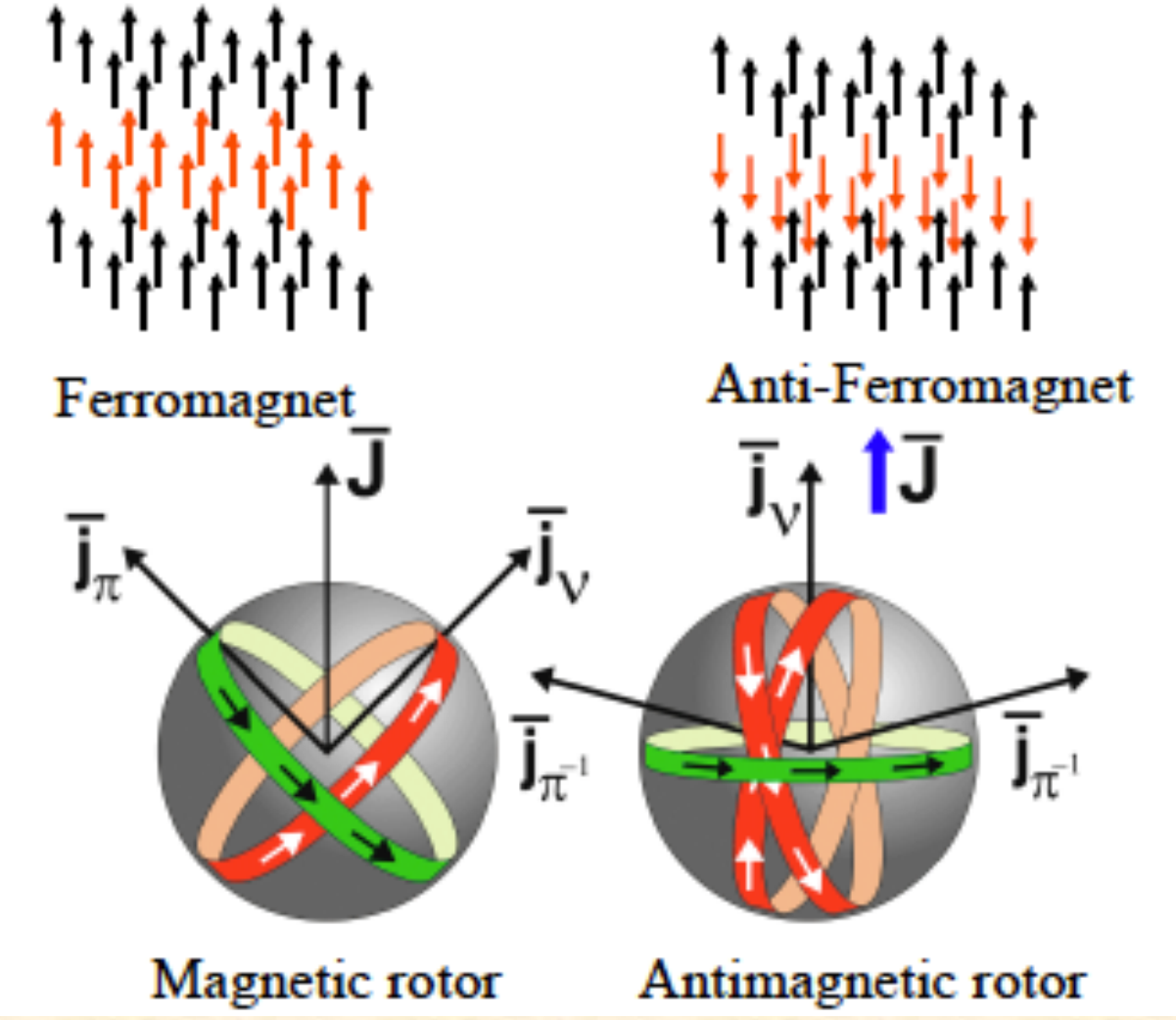

picture courtesy of S. Frauendorf

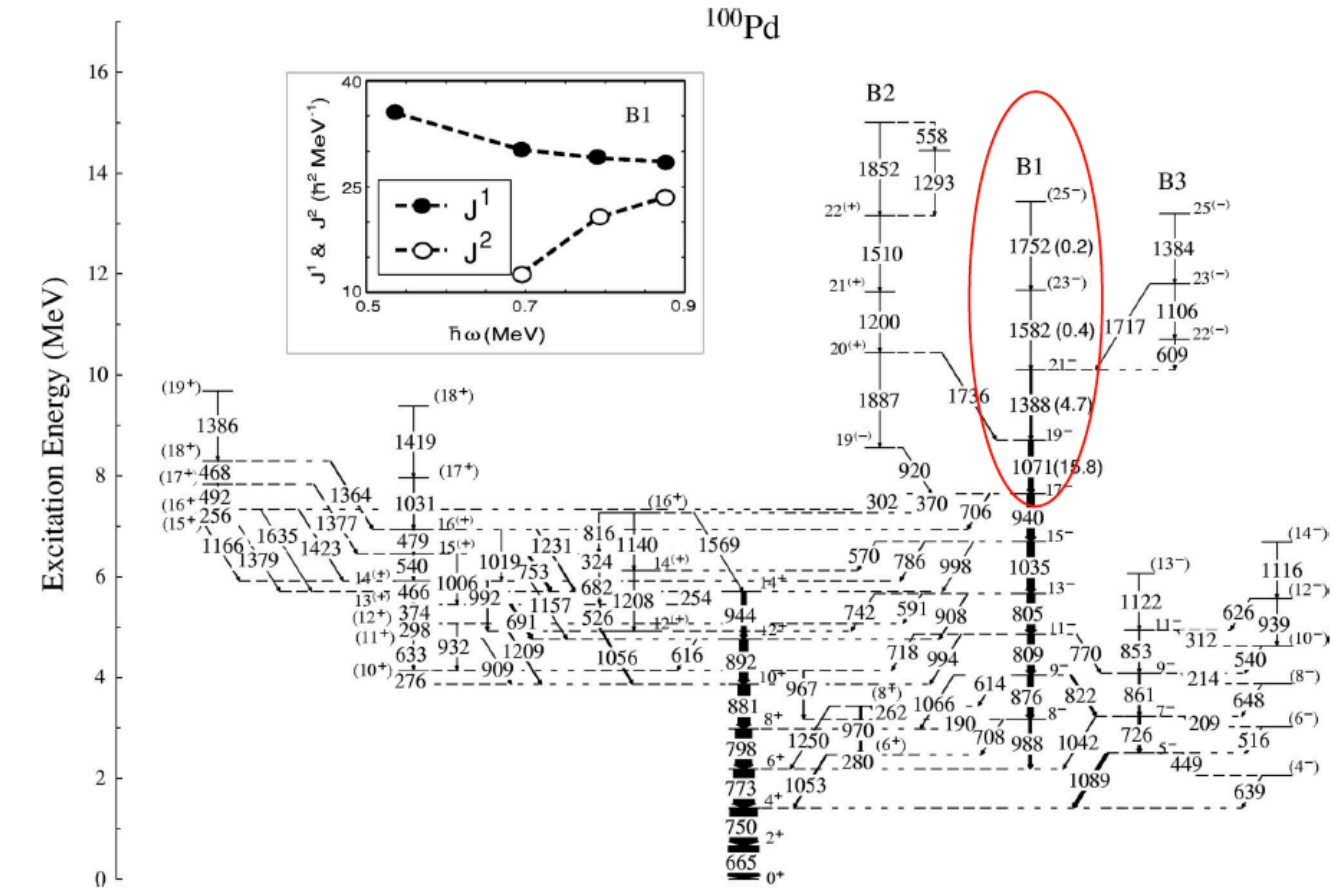

FIG. 2. Level scheme of ^{100}Pd obtained in this work. The widths of the arrows are proportional to the relative intensities of the transitions. For the transitions proposed as corresponding to antimagnetic rotation (AMR), intensities relative to the 665-keV line are given in parentheses next to the transition energies. In general, the uncertainties in transition energies are ~0.5 keV and in the intensities ~10%. The moments of inertia, $\mathcal{J}^{(1)}$ and $\mathcal{J}^{(2)}$, for the AMR transitions are shown in the inset.

S. Zhu *et al.*, Phys. Rev. C **64**, 041302 (R) (2001)

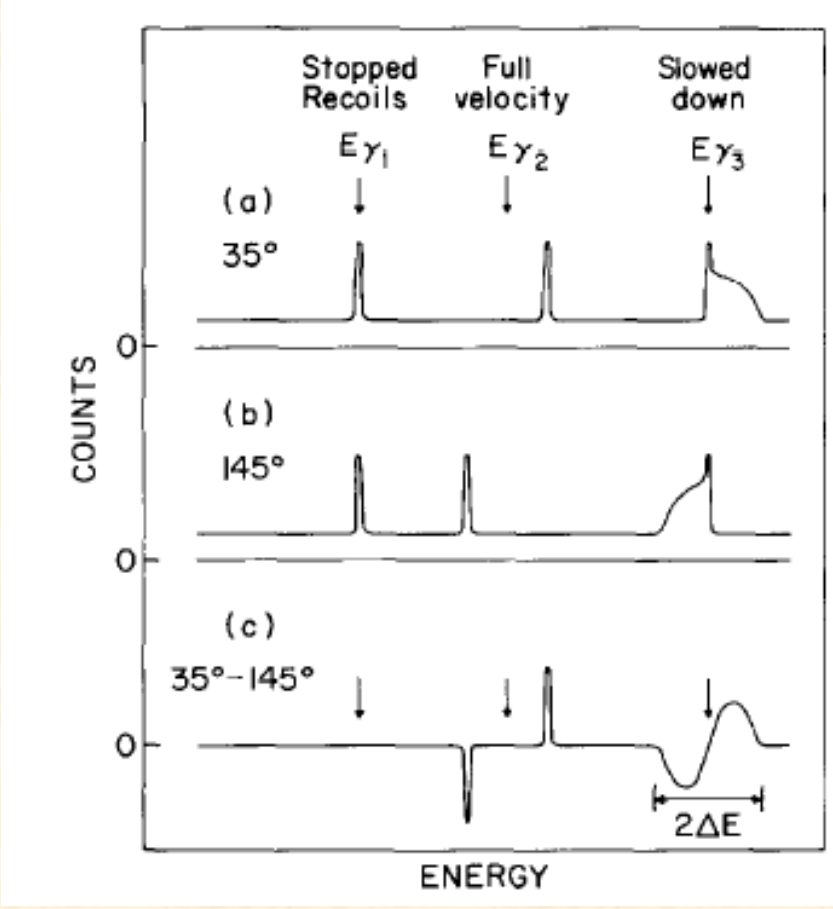

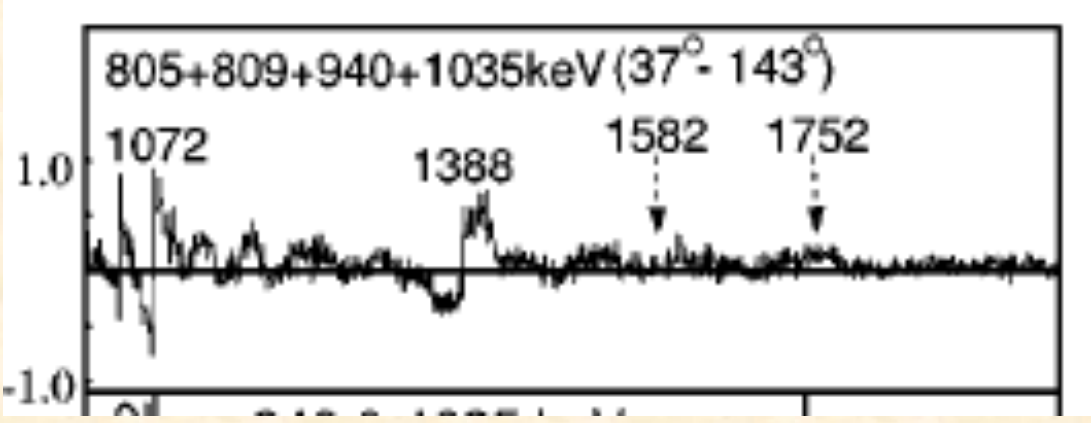

S. Zhu *et al.*, Phys. Rev. C **64**, 041302 (R) (2001)

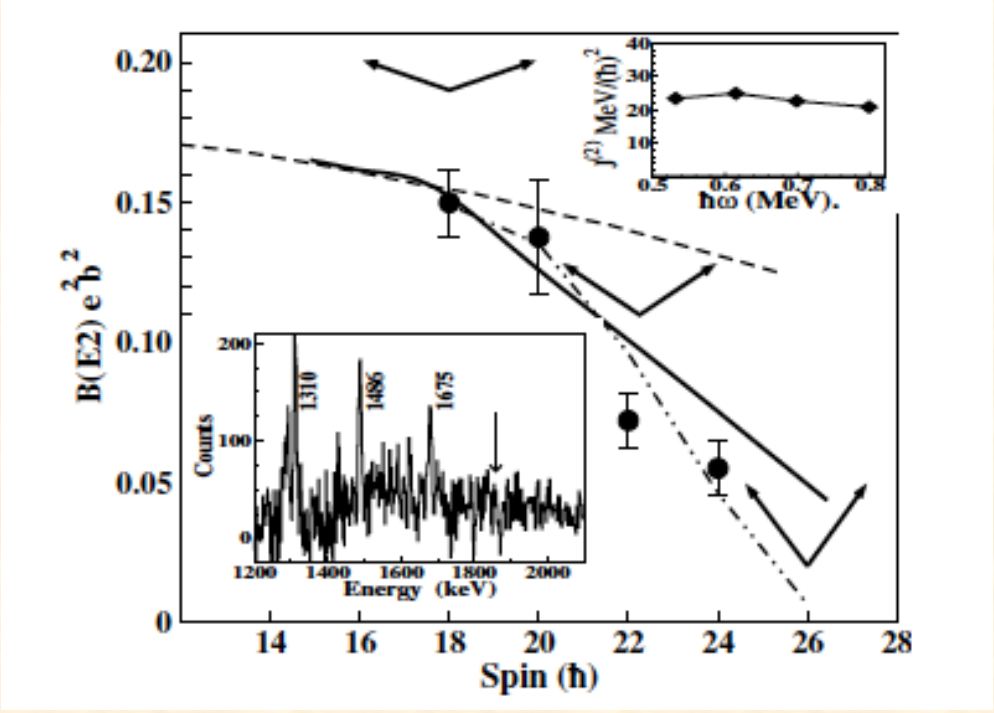

^{106}Cd

A.J. Simons *et al.*, Phys. Rev. Lett. **91**, 162501 (2003)

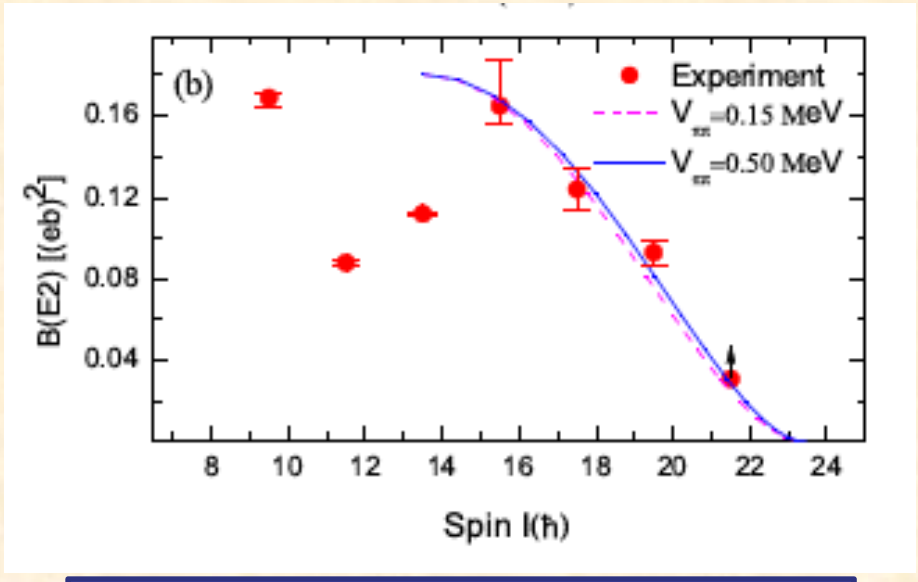

^{101}Pd

V. Singh *et al.*, J. Phys. G **44**, 075105 (2017)

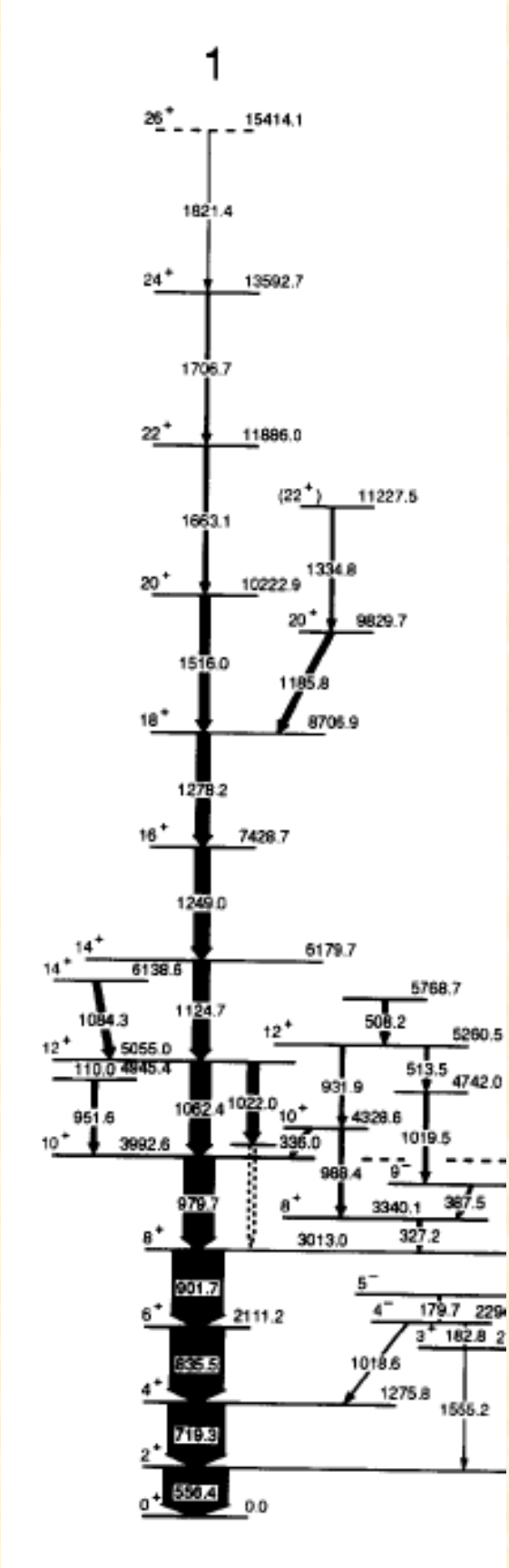
1
26+
15414.1
1821.4
24+
13592.7
1706.7
22+
11886.0
(22+)
11227.5
1653.1
1334.8
20+
10222.9
20+
9829.7
1516.0
1185.8
18+
8706.9
1278.2
16+
7428.7
1249.0
14+
6179.7
14+
6138.6
5768.7
1084.3
1124.7
508.2
12+
5260.5
12+
5055.0
110.0
4945.4
513.5
931.9
4742.0
951.6
1062.4
1022.0
10+
4328.6
10+
3992.6
336.0
1019.5
988.4
9−
979.7
8+
3340.1
387.5
8+
3013.0
327.2
901.7
5−
6+
2111.2
4−
179.7
229
3+
182.8
2
835.5
1018.6
4+
1275.8
1555.2
719.3
2+
550.4
0+
0.0

^{102}Pd

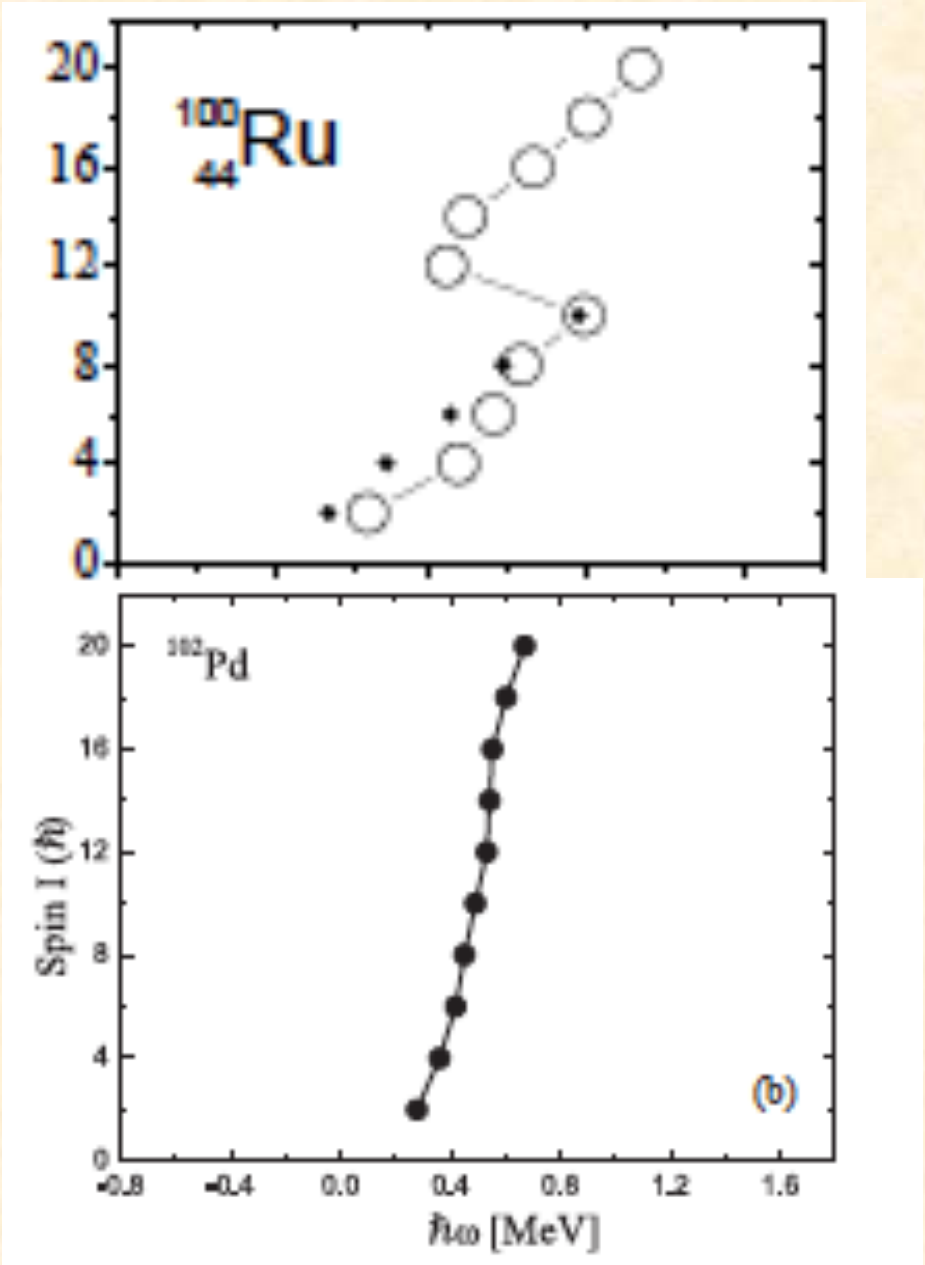

$E\gamma = [\,](4I - 2)$

$\hbar\omega \propto I$

S. Frauendorf, Y. Gu, and J. Sun,
Int. Mod. Phys. E 20, 465 (2011).

Tidal Waves in Nuclei:

The concept of nuclear tidal waves is based on the postulate that the yrast states (states of maximal angular momentum) in a phonon multiplet represent waves that travel over the nuclear surface akin to tidal waves over the ocean surface.

This nomenclature accounts for the observation that the yrast states in vibrational nuclei have a rotational-like structure for which a sound theoretical basis, especially at higher spins, has been lacking so far.

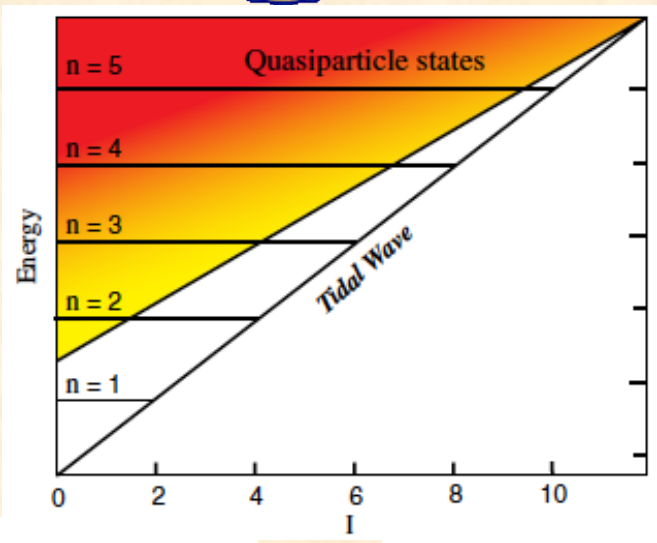

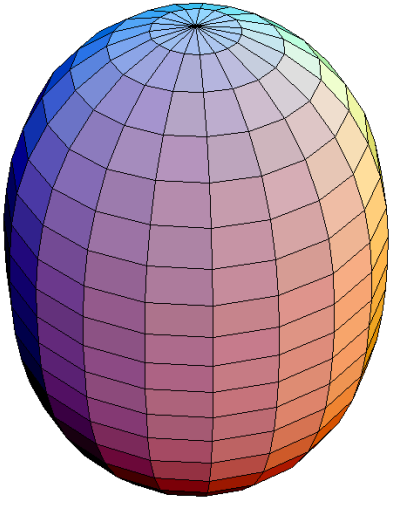

Minimal angular momentum

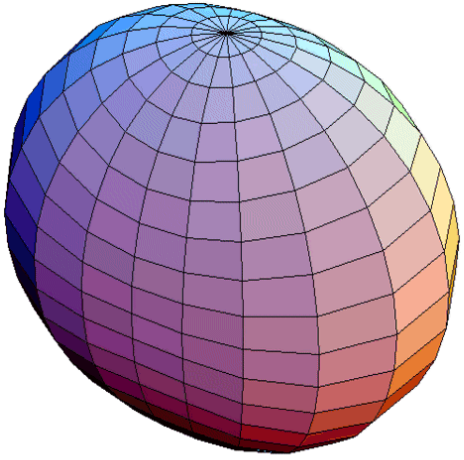

Maximal angular momentum

$$R(\vartheta,\varphi,t) = R_o\,[1+\beta\cos(\Omega t)Y_{20}(\vartheta,\varphi=0)]$$

$$R(\vartheta,\varphi,t) = R_o\,\left(1+\sqrt{2}\beta\sin\gamma\cos(2\varphi-\Omega t)Y_{22}(\vartheta,\varphi=0)\right)$$

animations courtesy of S. Frauendorf

In rigid rotation, the energy and angular momentum increase with increase in frequency; the shape (moment of inertia) remains unchanged.

B(E2) ~ Constant

In tidal wave, the energy and angular momentum increase with the amplitude of the wave (change in shape); the frequency remains constant.

B(E2) ➔ J

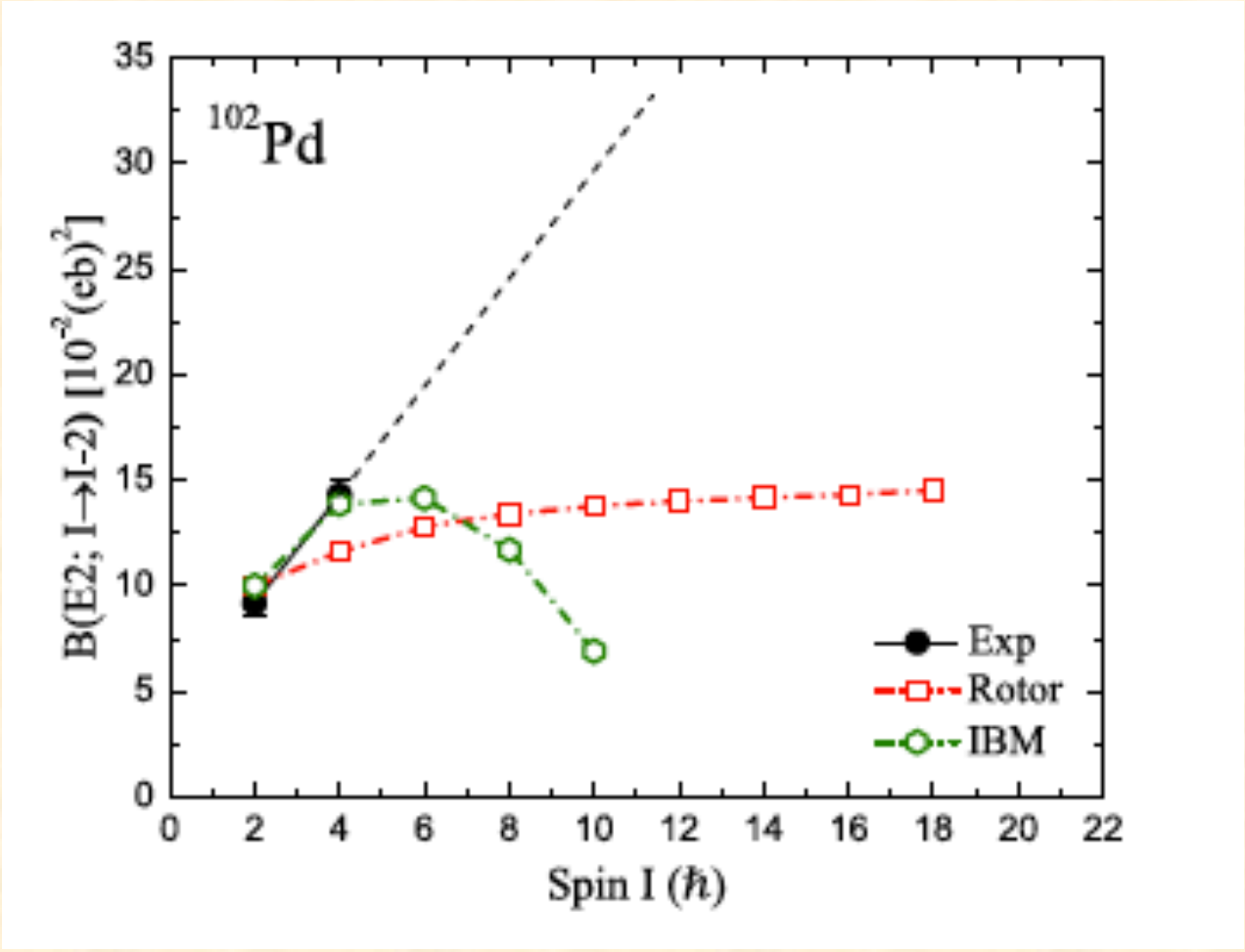
^{102}Pd
B(E2; I→I-2) [10^{-2}(eb)^2]
Spin I ($\hbar$)
Exp
Rotor
IBM
0
5
10
15
20
25
30
35
0
2
4
6
8
10
12
14
16
18
20
22

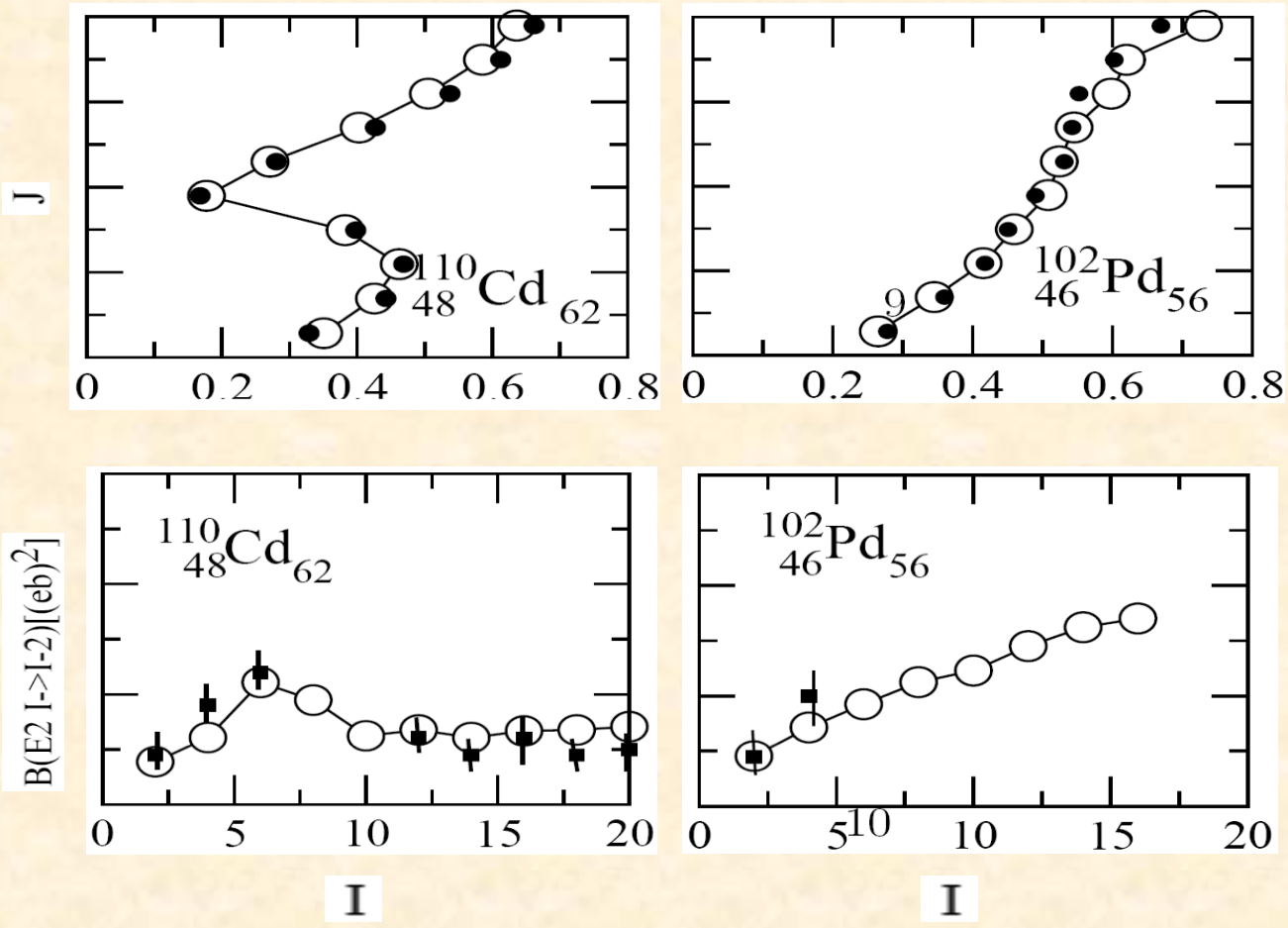

S. Frauendorf, Y. Gu, and J. Sun,
Int. Mod. Phys. E 20, 465 (2011).

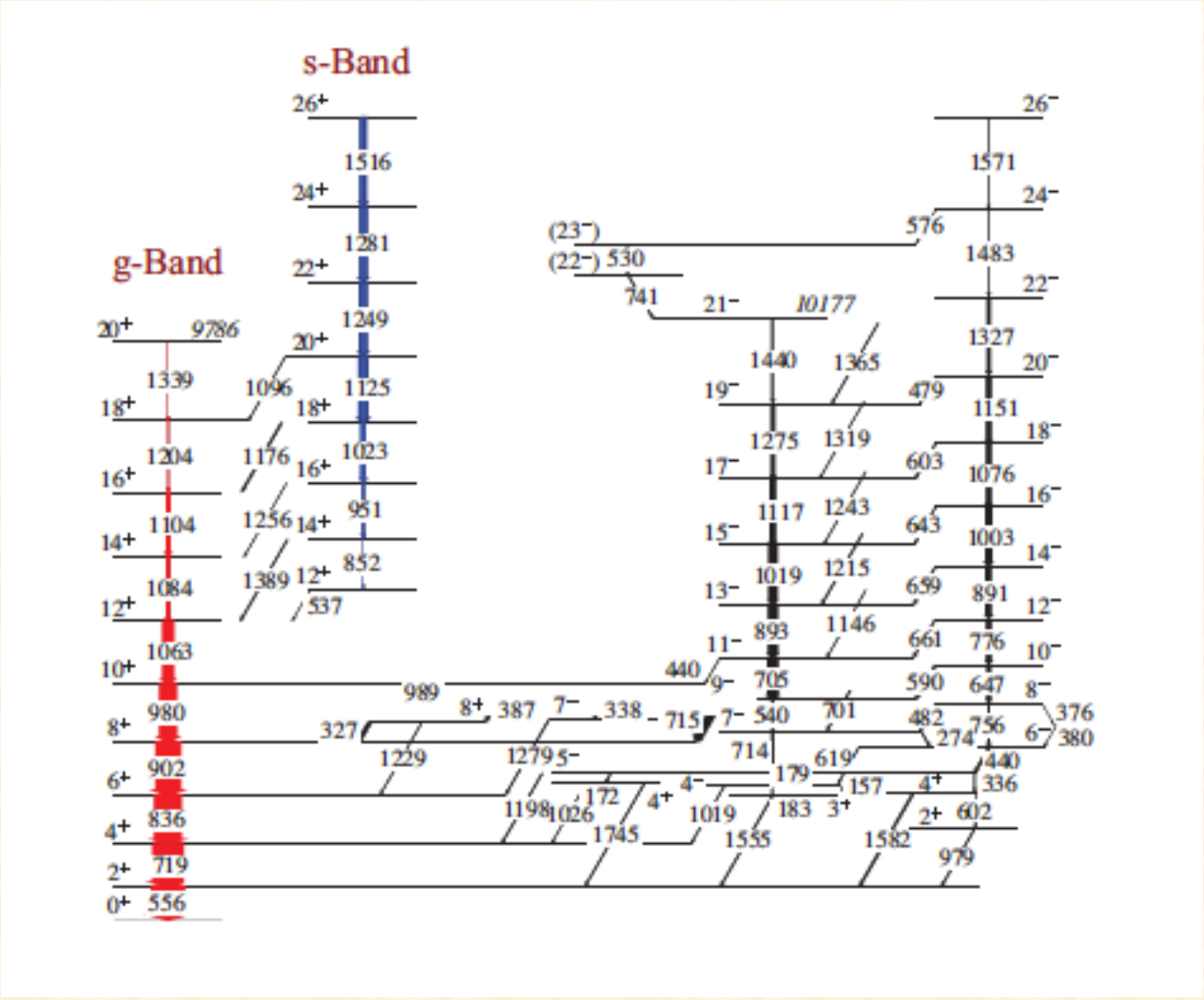
s-Band
g-Band
26+
1516
24+
1281
22+
1249
20+
1125
18+
1023
16+
951
14+
852
12+
537
20+ 9786
1339
18+
1204
16+
1104
14+
1084
12+
1063
10+
980
8+
902
6+
836
4+
719
2+
556
1096
1176
1256
1389
989
327
1229
8+ 387
7− 338
1279
5−
1198
1026
172
4+
1745
(23−)
(22−) 530
741
21− 10177
1440
1365
19−
479
1275
1319
17−
603
1117
1243
15−
643
1019
1215
13−
659
893
1146
11−
661
440
9−
705
590
715
7− 540
701
482
714
619
179
4−
157
4+
1019
183
3+
1555
1582
2+ 602
979
26−
1571
24−
576
1483
22−
1327
20−
479
1151
18−
603
1076
16−
643
1003
14−
659
891
12−
661
776
10−
590
647
8−
482
756
6−
376
274
380
440
336

^{102}Pd

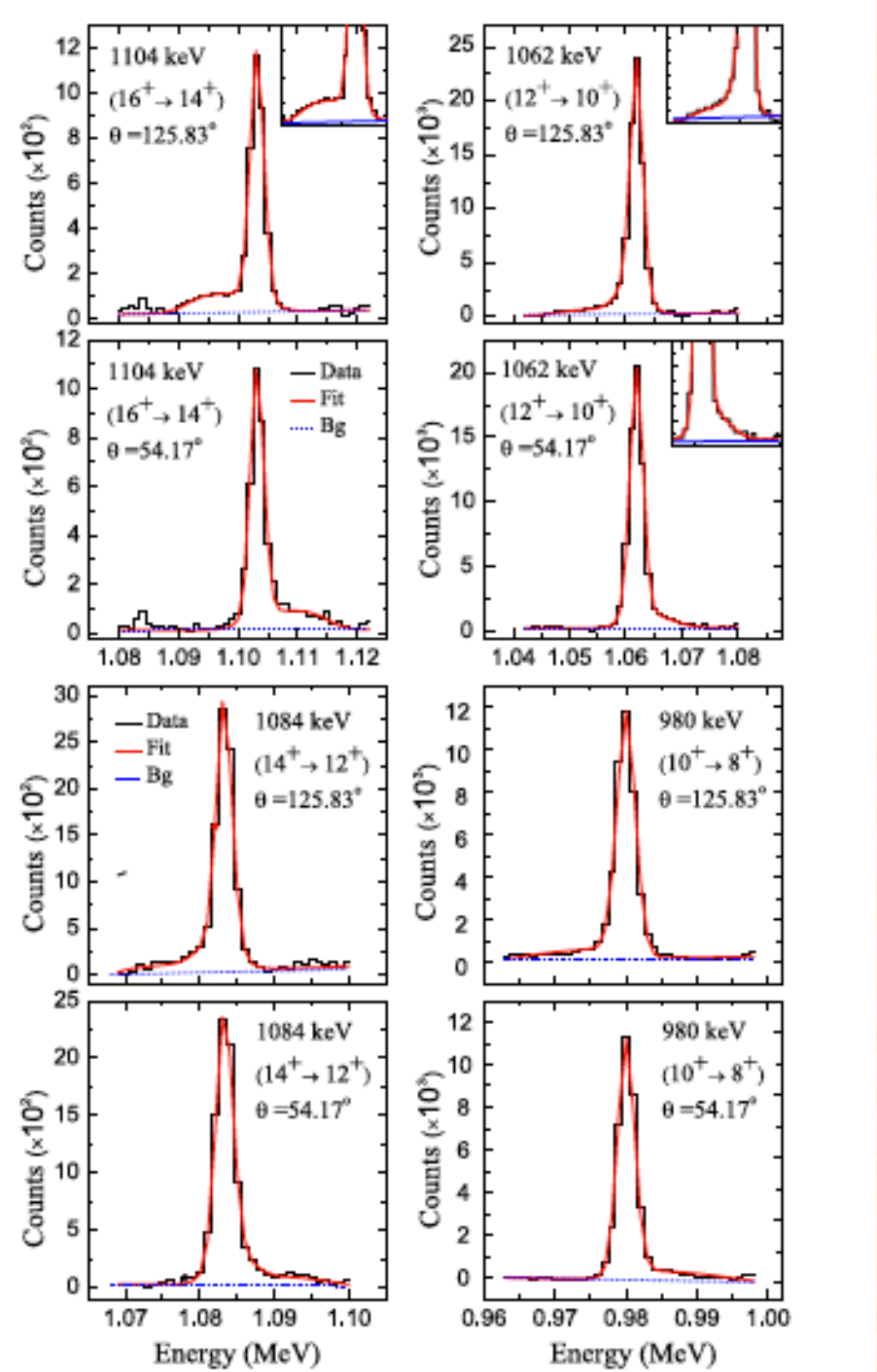

A. D. Ayangeakaa *et al.*,
Phys. Rev. Lett. 110, 102501 (2013)

MEASURED LIFETIMES AND ELECTROMAGNETIC TRANSITION PROBABILITIES FOR THE YRAST BAND IN ^{102}Pd.

E_γ(MeV)	$I_i^\pi \rightarrow I_f^\pi$	τ(ps)	$B(E2)(e^2b^2)$	Q_t(eb)
0.836	$6^+ \rightarrow 4^+$	1.15(32)	0.174(48)	2.36(33)
0.902	$8^+ \rightarrow 6^+$	0.720(42)	0.190(11)	2.41(07)
0.980	$10^+ \rightarrow 8^+$	0.409(28)	0.221(15)	2.56(09)
1.062	$12^+ \rightarrow 10^+$	0.252(18)	0.240(17)	2.65(09)
1.083	$14^+ \rightarrow 12^+$	0.201(11)	$0.272(^{+15}_{-22})$	$2.80(^{+08}_{-13})$
1.104	$16^+ \rightarrow 14^+$	0.180(21)[2]	$0.277(^{+33}_{-42})$	$2.81(^{+17}_{-21})$

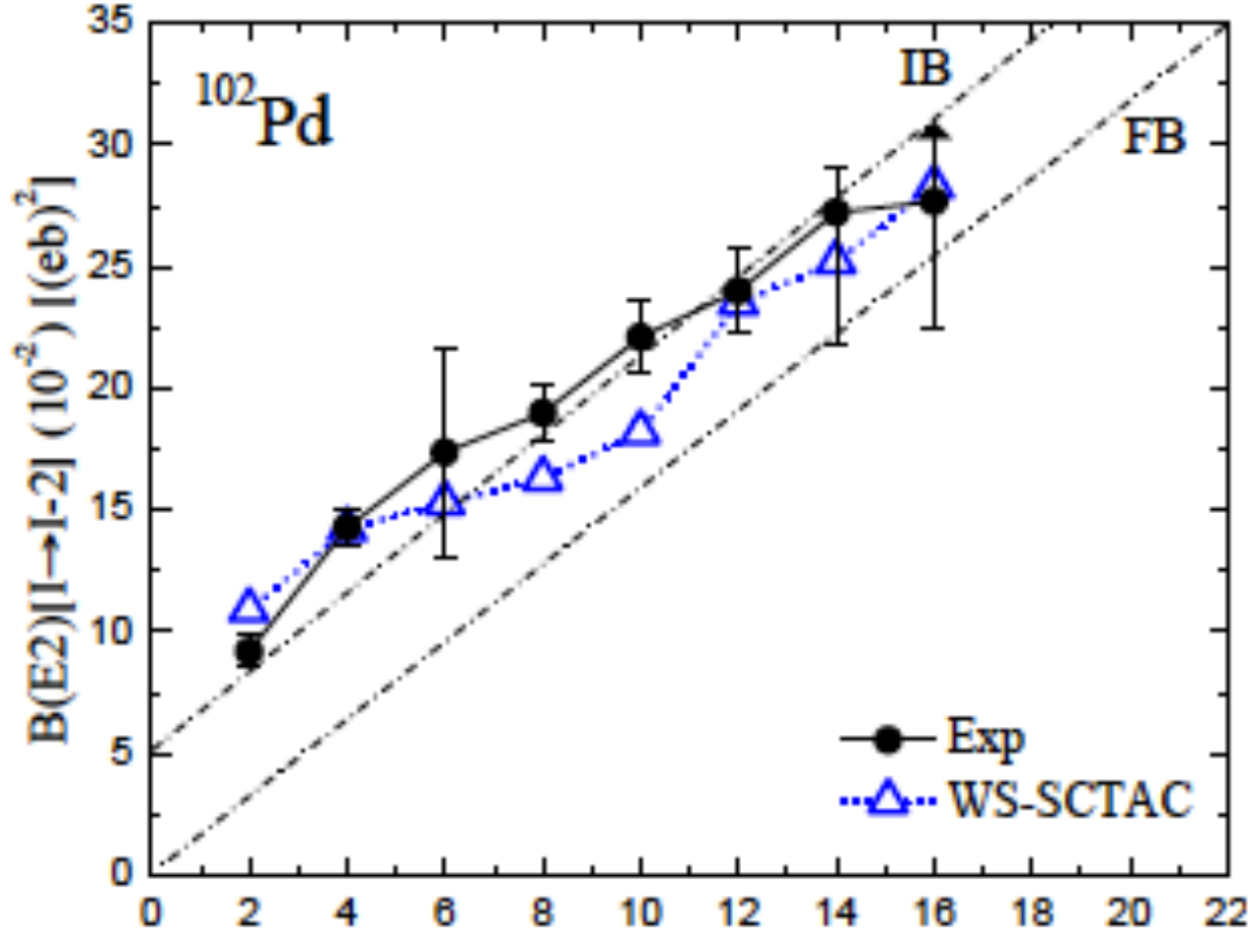

A. D. Ayangeakaa *et al.*,
Phys. Rev. Lett. 110, 102501 (2013)

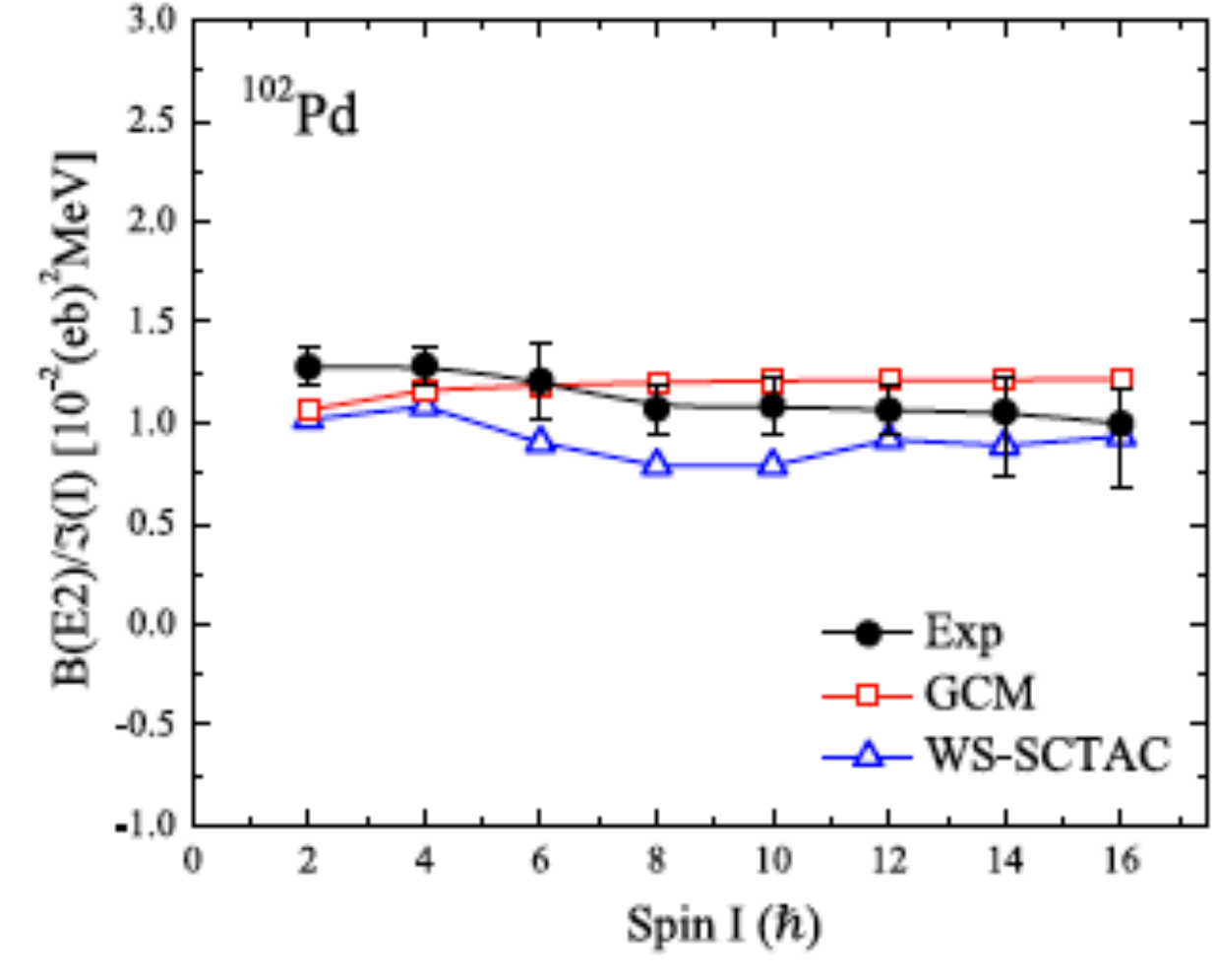
^{102}Pd
B(E2)/3(I) [10^{-2}(eb)^{2}MeV]
Spin I ($\hbar$)
Exp
GCM
WS-SCTAC
3.0
2.5
2.0
1.5
1.0
0.5
0.0
-0.5
-1.0
0
2
4
6
8
10
12
14
16

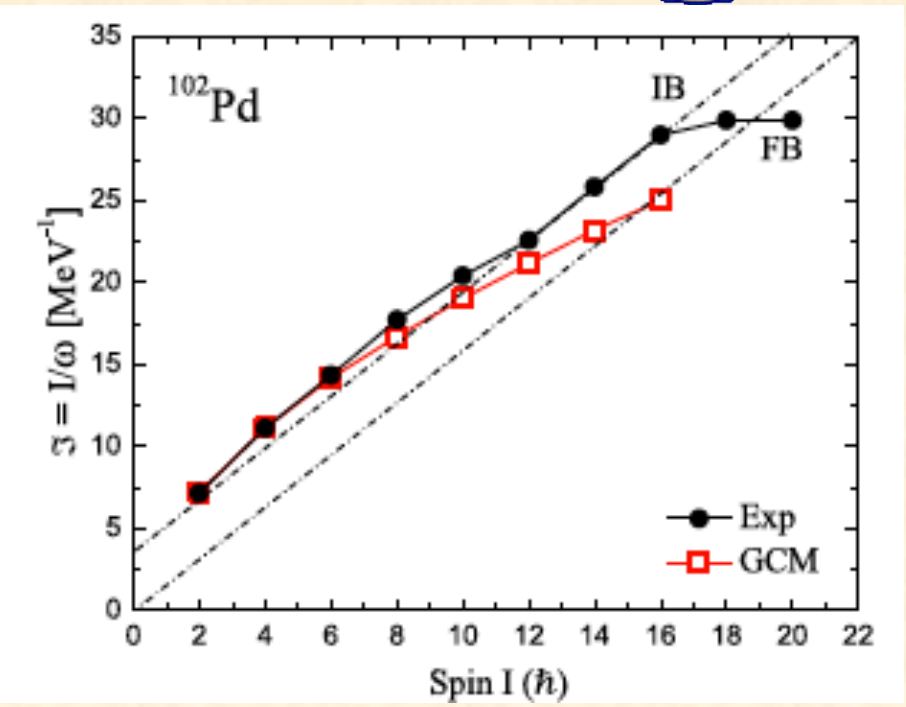
^{102}Pd
IB
FB
Exp
GCM
$\Im = I/\omega$ [MeV^{-1}]
Spin I ($\hbar$)

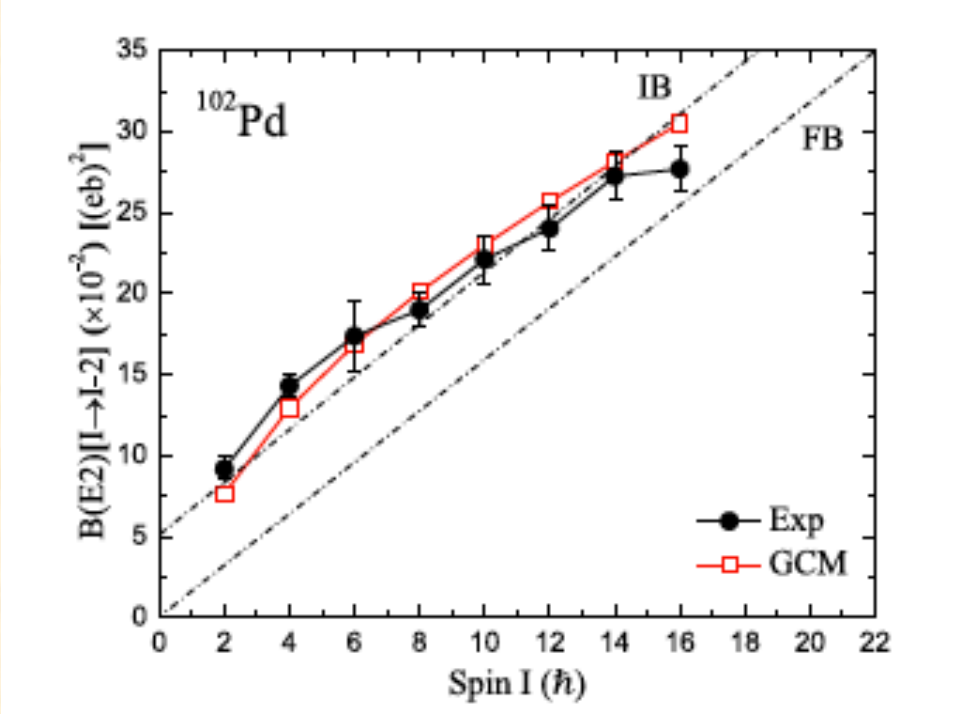
^{102}Pd
IB
FB
Exp
GCM
B(E2)[I→I-2] (×10^{-2}) [(eb)^2]
Spin I ($\hbar$)

In the simplest approximation of pure harmonic motion, the energy and the angular momenta of the yrast states is given by:

$$E_n = n\omega_0 \qquad I = 2n \tag{1}$$

where *n* is the number of phonons with energy ω_0.

It is of interest to consider the effects of anharmonic terms [3,4] arising from the interaction between phonons. To lowest order, Eq. (1) gets modified as follows:

$$E_n \approx n\omega_0 + \frac{1}{2}V_0 n(n-1) + \ldots \tag{2}$$

Eq. (2) can be rewritten in terms of angular momentum:

$$E(I) \approx (\frac{\omega_0}{2} - \frac{V_0}{4})I + \frac{1}{8}V_0 I^2 + \ldots$$

$$E(I) \approx aI + bI^2 + \ldots$$

from which the rotational frequency and the moment of inertia can be derived

$$\omega = \frac{\partial E(I)}{\partial I} \approx a + 2bI + \ldots$$

$$\Im = \frac{I}{\omega} \approx \frac{I}{a + 2bI} \qquad (3)$$

Along the same lines, the transition probabilities can be parametrized in the form [4]:

$$B(E2) \approx cI + dI^2 + eI^3 + \ldots \qquad (4)$$

A.O. Macchiavelli *et al.*,
Phys. Rev. C **90**, 047304 (2014).

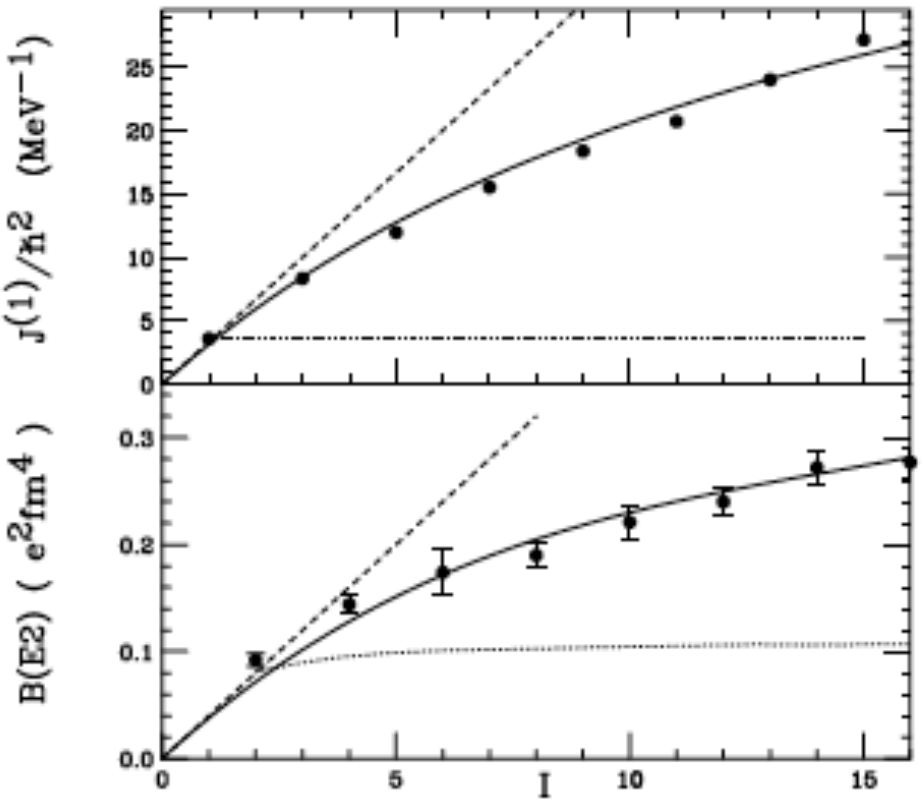

FIG. 1. Top: Moment of inertia in the yrast band in ^{102}Pd and the results of Eq. (5). Bottom: $B(E2)$ values and Eq. (6). The harmonic and rotational limits are shown in dashed and dotted lines

A.O. Macchiavelli *et al.*,
Phys. Rev. C **90**, 047304 (2014).

✓Measured B(E2)'s of the yrast band in ^{102}Pd vary linearly with spin

conforms to expectation from a tidal wave picture

rotating condensate of 7 aligned d-bosons

✓ Alternative explanation in terms of GCM cannot simultaneously describe both energies and B(E2)'s.

✓ A simple phenomenological phonon model, with anharmonic terms reproduces the observed data, providing an independent confirmation of the multi-phonon picture associated with tidal waves..

A.D. Ayangeakaa *et al.*,
Phys. Rev. Lett. **110,** 102501 (2013).

A.O. Macchiavelli *et al.*,
Phys. Rev. C **90**, 047304 (2014).

What is Chirality?

The word chiral comes from the Greek "*chaire*" (hand).
So, "Chirality" stands for "handedness"

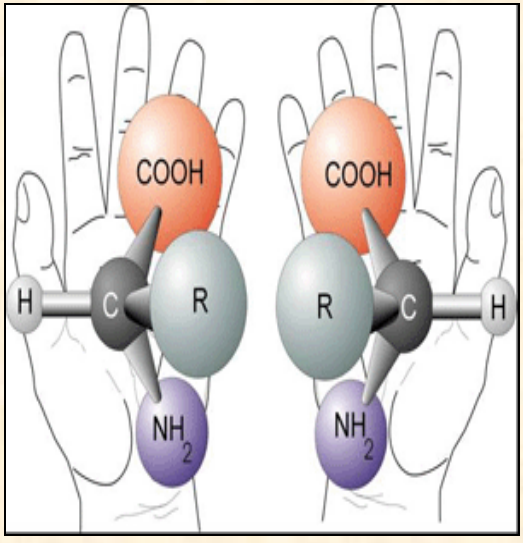

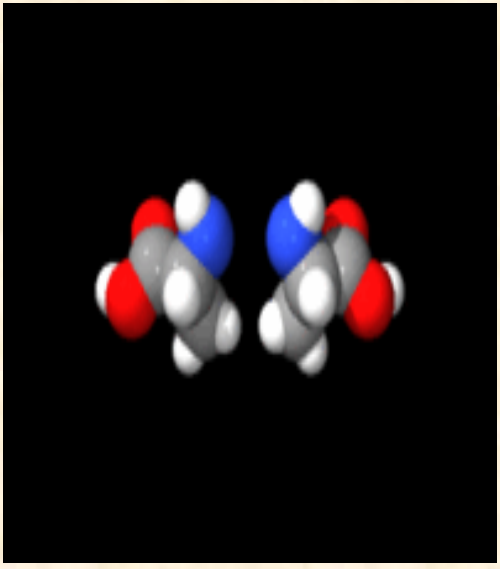

Chirality is quite common in nature:

All terrestrial life uses only right-handed sugars and left-handed amino acids.

More than 50 percent of the world's top 100 drugs are chiral, including familiar brand names such as Lipitor, Paxil, Zoloft and Nexium.

The classic, tragic example is the sedative thalidomide, made infamous during the 1960s. Though thalidomide's right-handed enantiomer helped fight morning sickness in pregnant women, its left-handed version caused severe birth defects.

In the case of the common pain-reliever ibuprofen, the molecule's right-handed version is simply 100 times less powerful than its left-handed twin.

Chirality in Nuclei

γ-deformation, $\gamma \sim 30^{o}$

$\mathcal{I}_s \sim \mathcal{I}_l < \mathcal{I}_i$

Configurations

Particles: short-axis

Holes: long-axis

Core: intermediate-axis

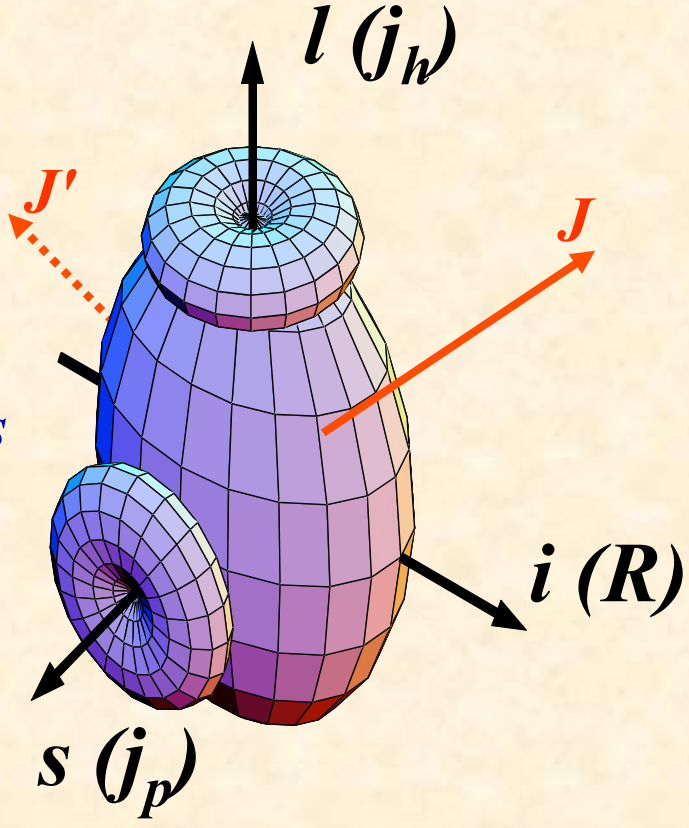

The left-handed configuration is converted into the right handed one by the time reversal operation

picture courtesy of S. Zhu

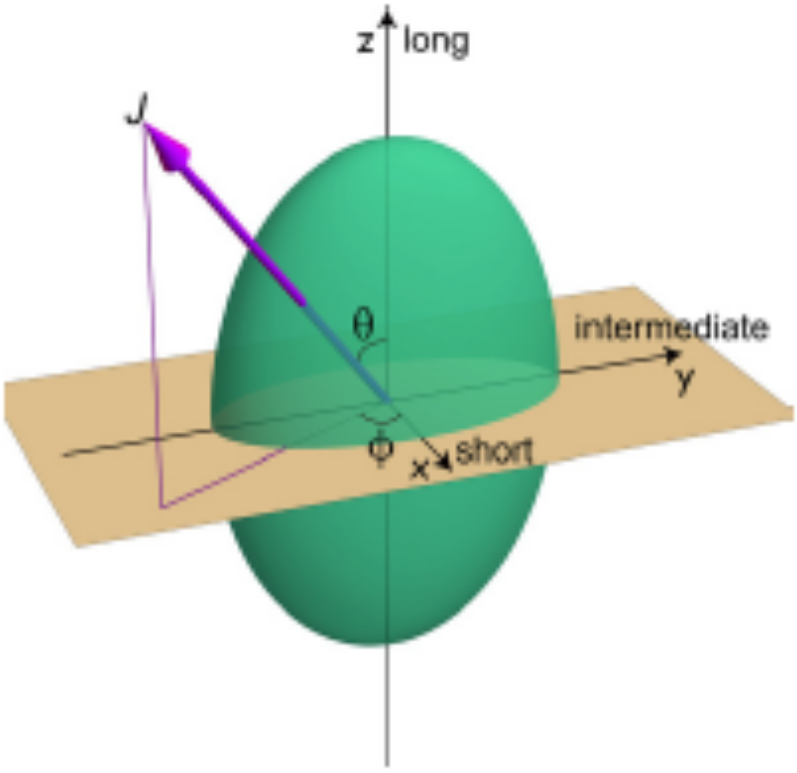

Fig. 1. (Color online.) A schematic picture for the aplanar rotation of a triaxial nucleus. The arrow $\boldsymbol{J}$ denotes the total angular momentum vector, and the short, intermediate, and long axes are denoted by x, y, and z, respectively.

P. W. Zhao, Phys. Lett. B **773**, 1 (2017)

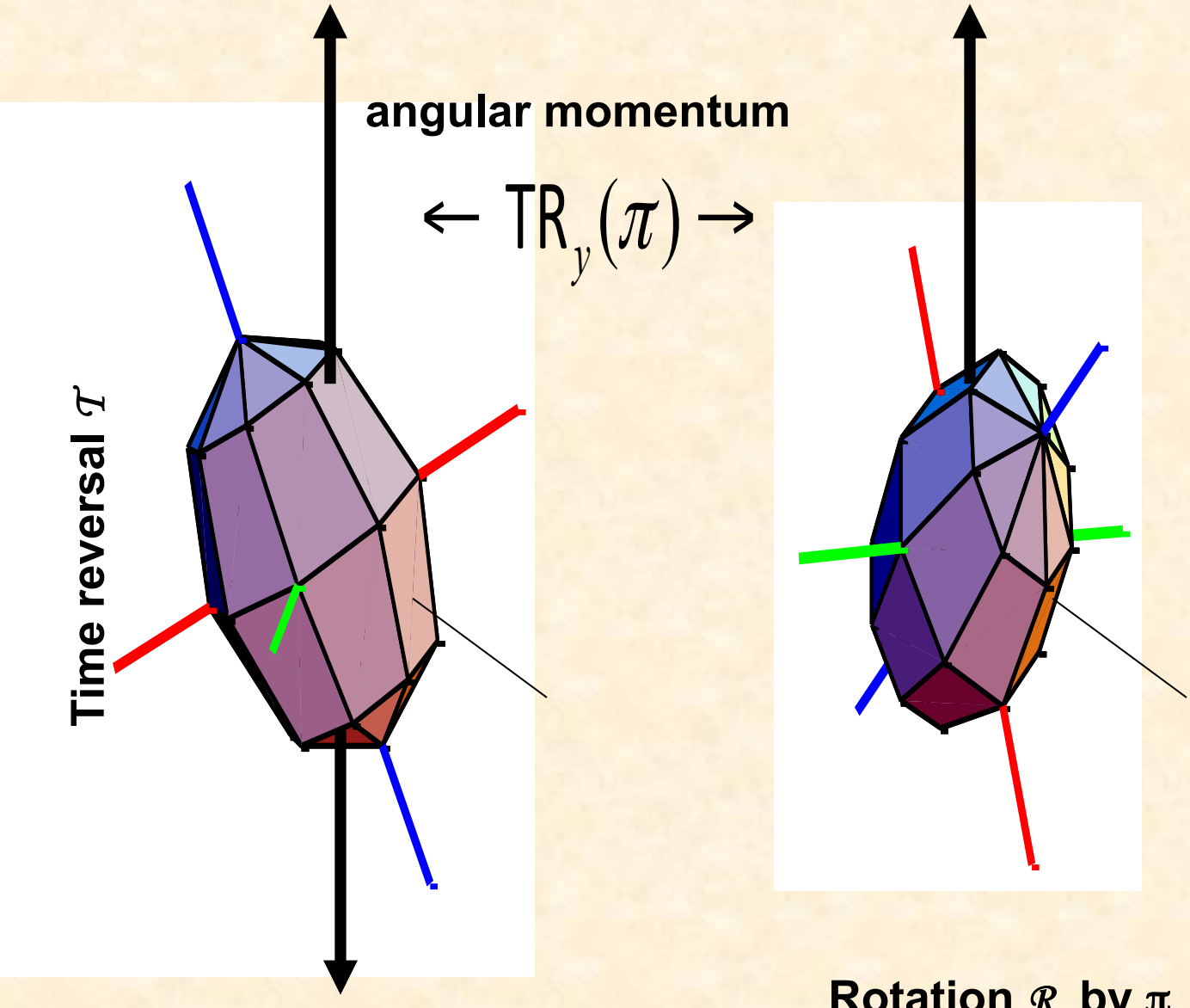

animations courtesy of S. Frauendorf

A Triaxial Nucleus becomes Chiral if it rotates about an axis that lies outside the three planes spanned by the principal axes of it's triaxial ellipsoidal shape.

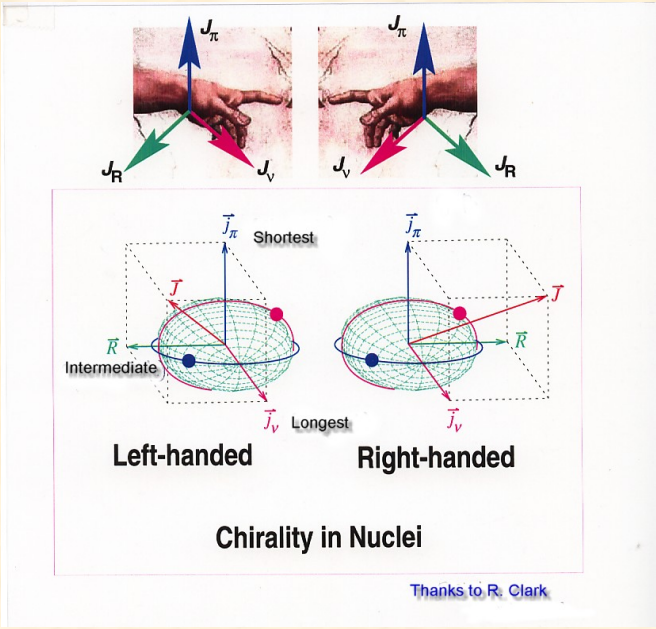

Two exactly identical bands with same Energy and Parity De-excitation of the partner bands in a very similar way via Electromagnetic radiation

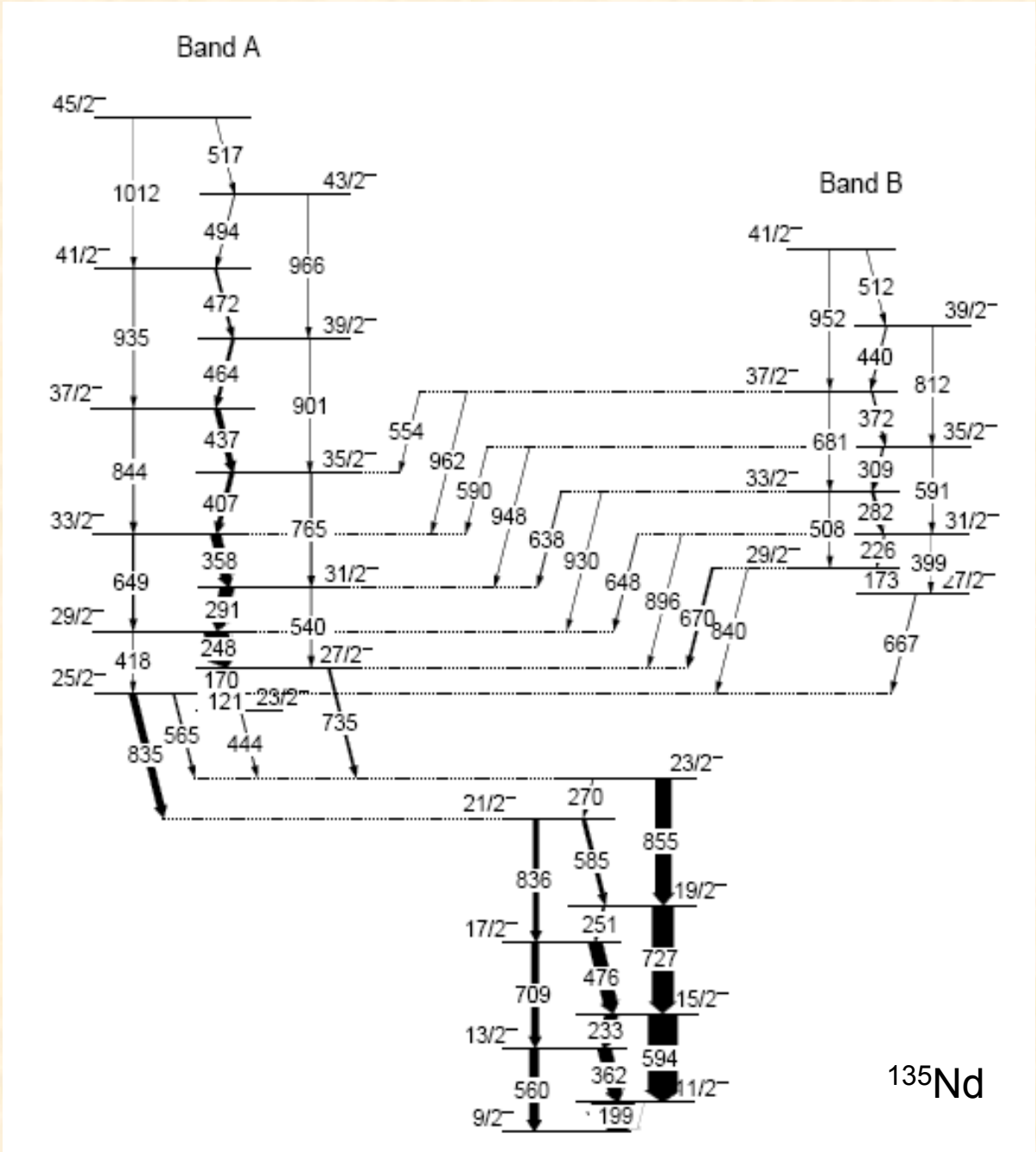

S. Zhu *et al.*, Phys. Rev. Lett. **91**, 132501 (2003)

3D TAC Results

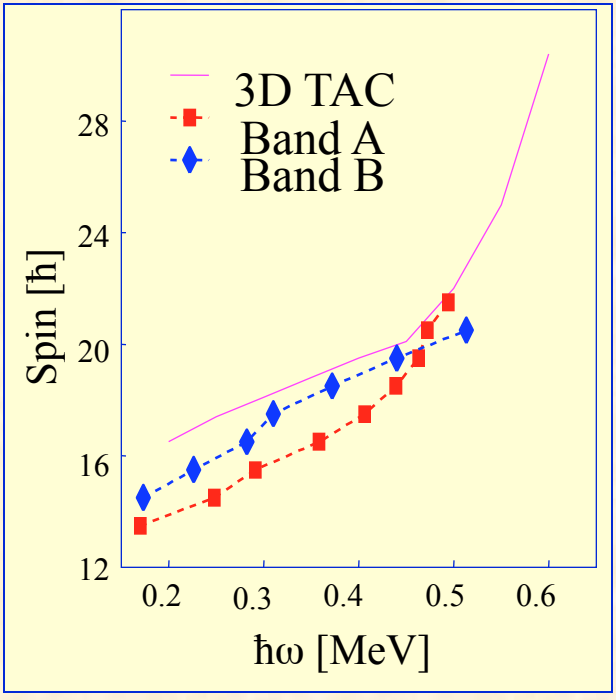

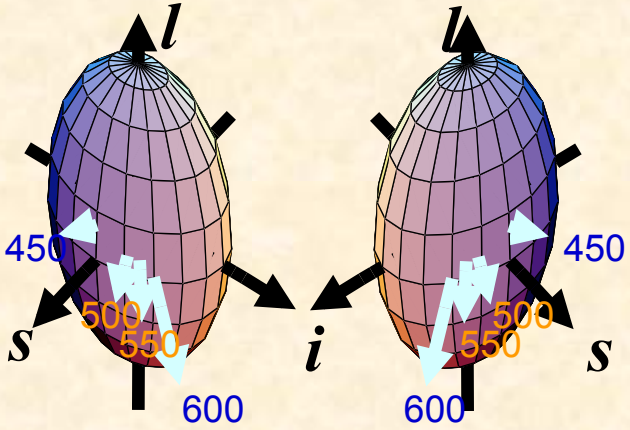

$\hbar\omega$[MeV]	ϑ	φ	$I(\omega)$[ħ]
0.45	65°	0°	20.1
0.50	75°	28°	22.0
0.55	75°	37°	25.0
0.60	85°	47°	30.4

$\pi(h_{11/2})^2\ \nu(h_{11/2})^{-1}$

^{135}Nd

S. Zhu *et al.*, Phys. Rev. Lett. **91**, 132501 (2003)

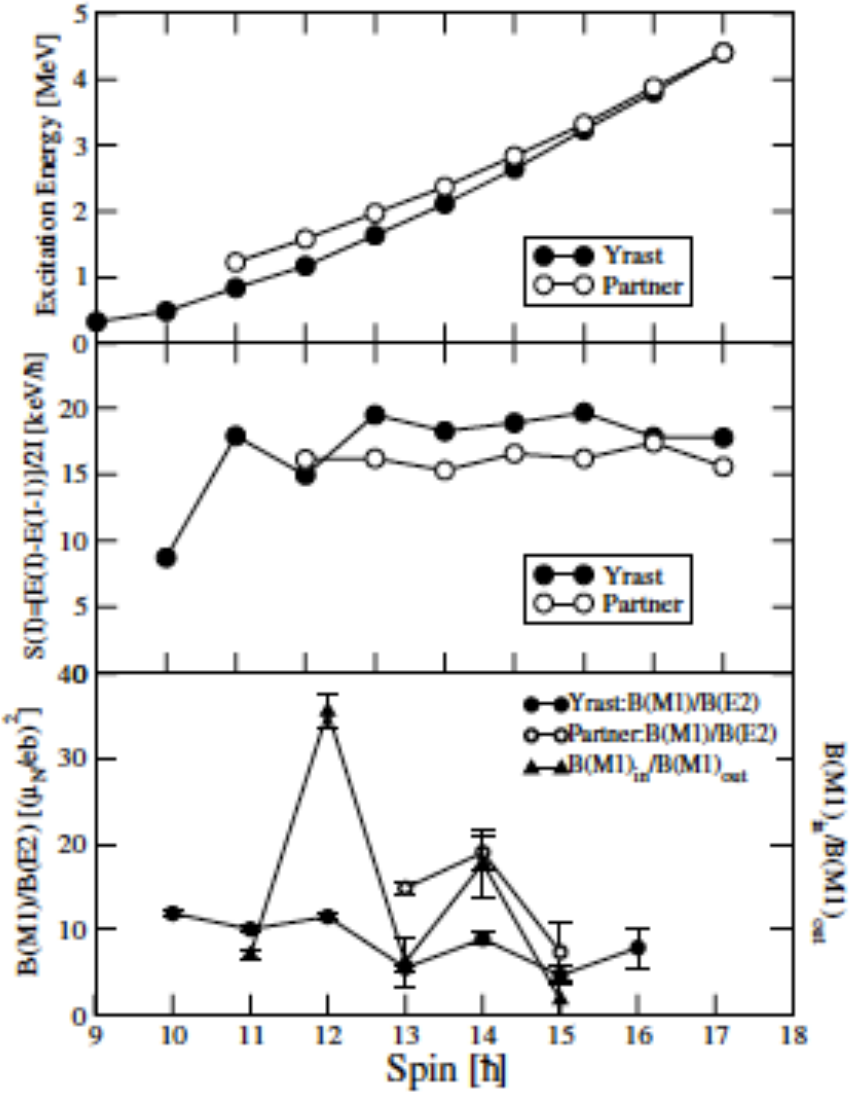

FIG. 3. Chiral fingerprints: (a) excitation energy vs spin; (b) $S(I)$ vs spin; (c) $B(M1)/B(E2)$ and $B(M1)_{\text{in}}/B(M1)_{\text{out}}$.

^{104}Rh

C. Vaman *et al.*, Phys. Rev. Lett. **92**, 032501 (2004)

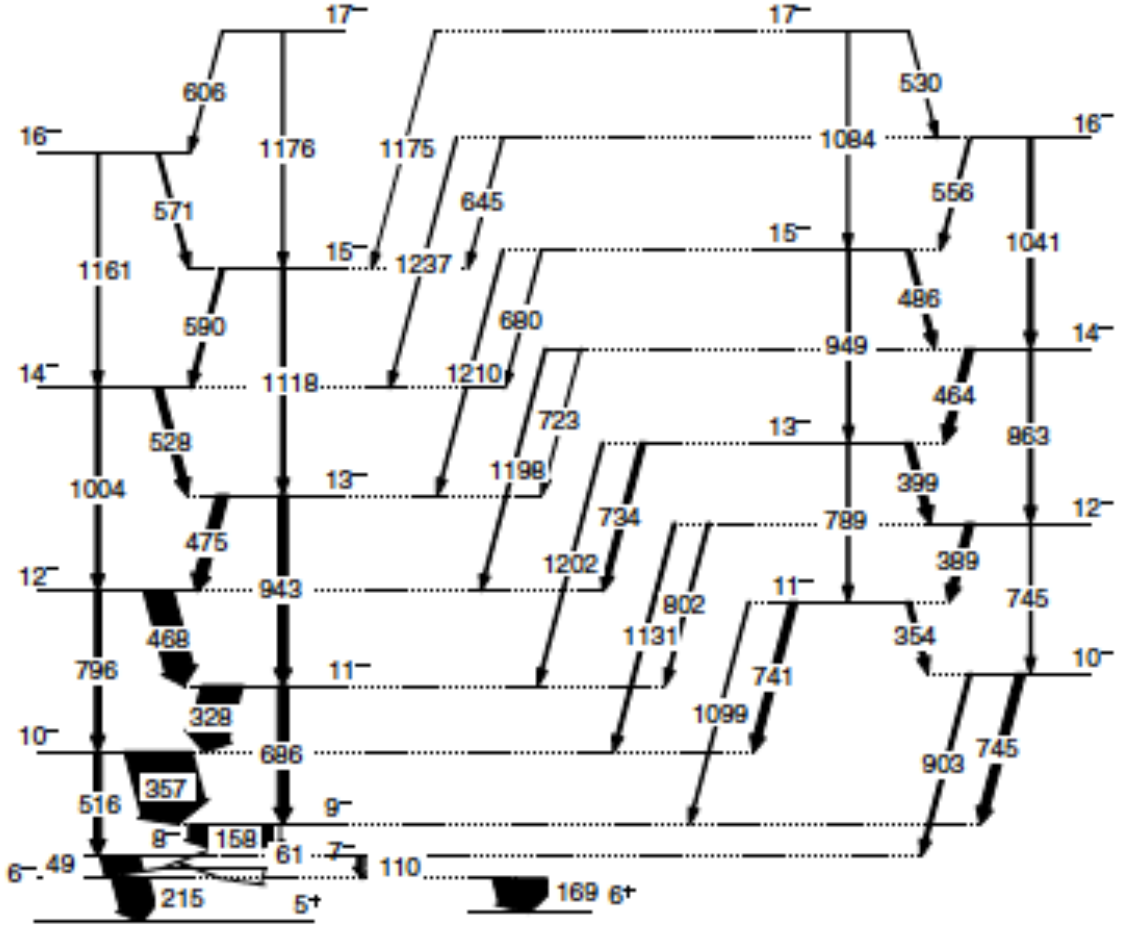

FIG. 2. Partial level scheme showing the $\pi g_{9/2} \otimes \nu h_{11/2}$ chiral bands in ^{104}Rh.

C. Vaman *et al.*, Phys. Rev. Lett. **92**, 032501 (2004)

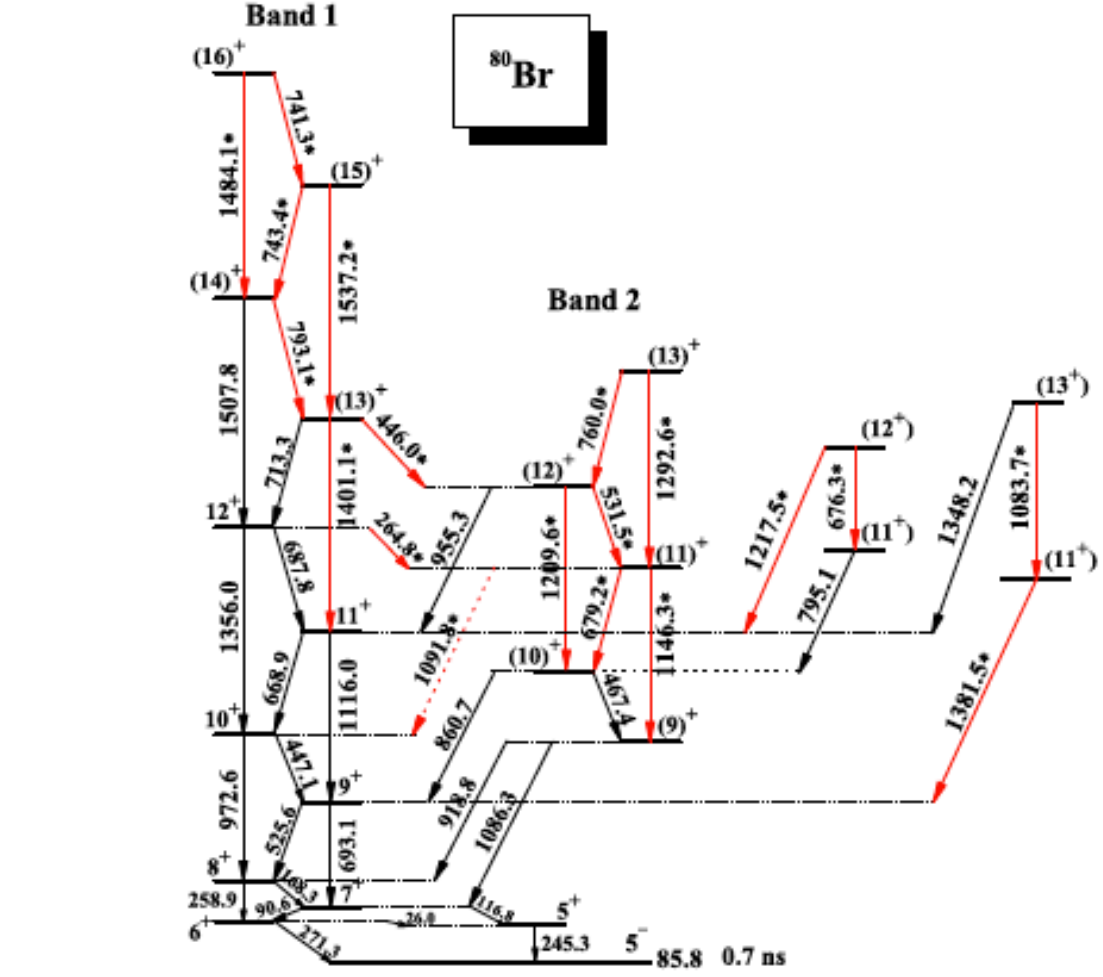

Fig. 1. (Color online.) Partial level scheme for ^{80}Br obtained in the present work. New observed transitions are indicated by stars and red lines.

S.Y. Wang *et al.*, Phys. Lett. B **703**, 40 (2011)

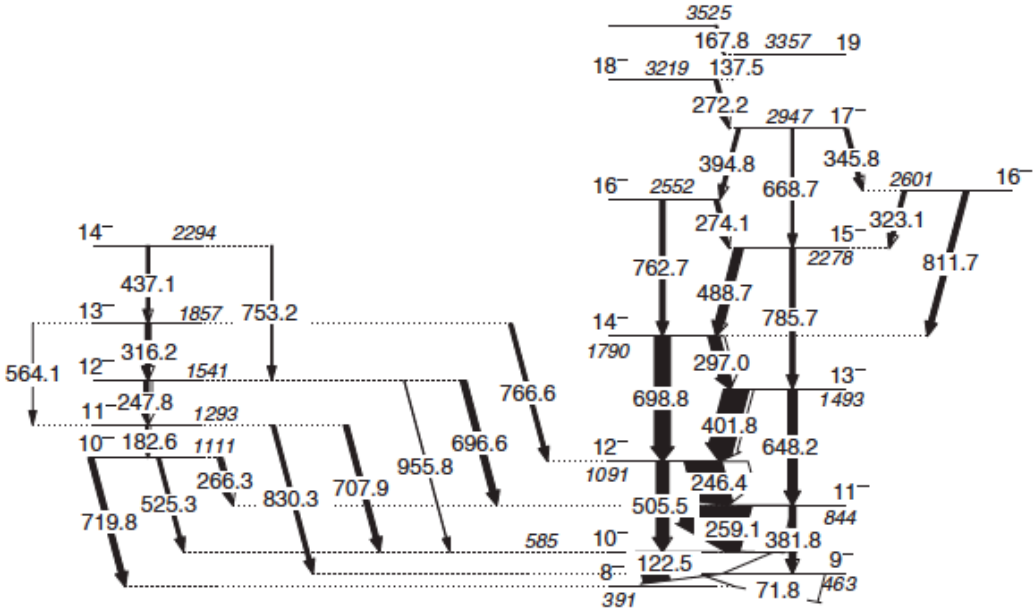

FIG. 1. Partial level scheme showing the pair of bands in ^{198}Tl.

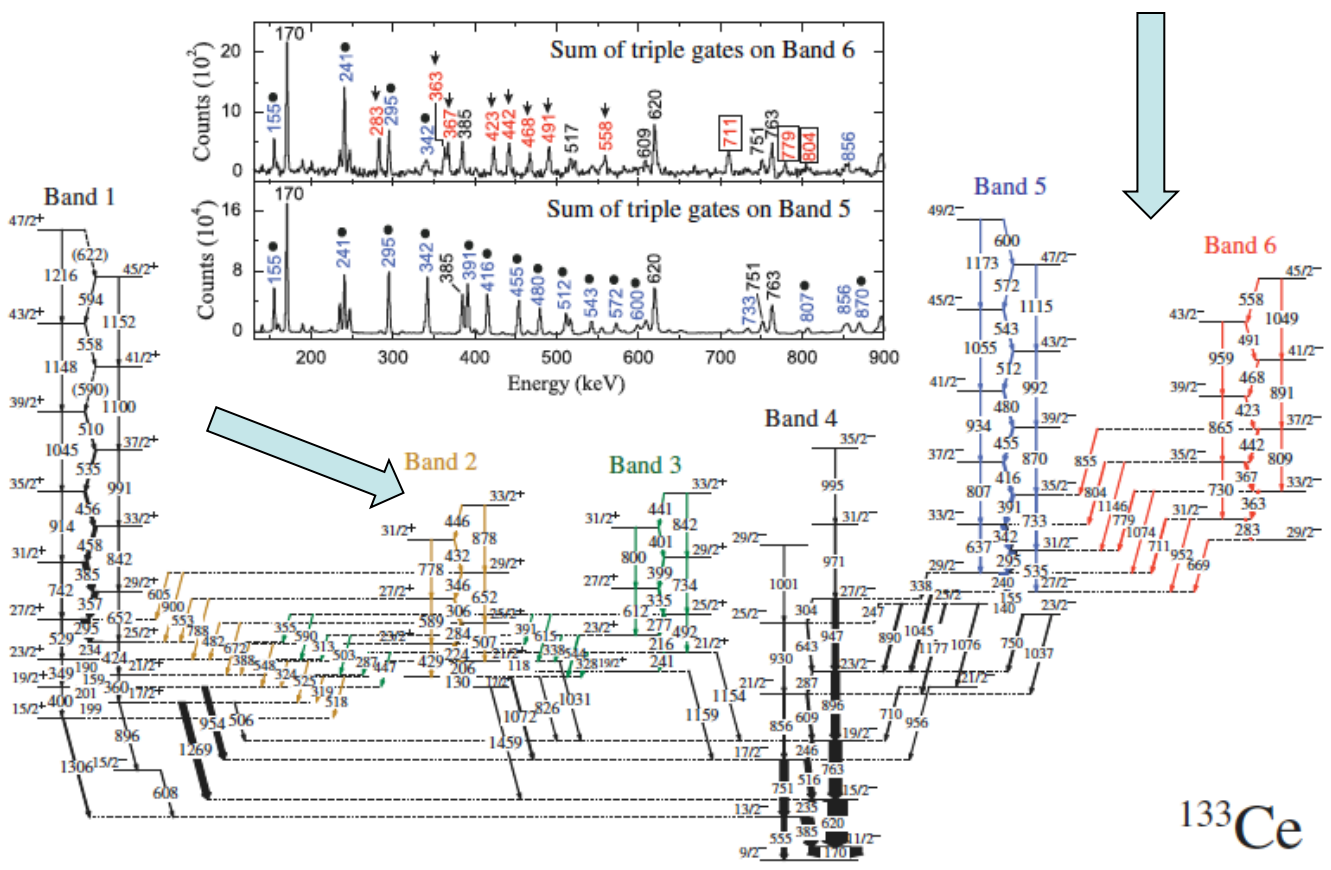

$$\pi[(1g_{7/2})^{-1}(1h_{11/2})^{1}] \otimes \nu(1h_{11/2})^{-1}$$
$$\pi(1h_{11/2})^{2} \otimes \nu(1h_{11/2})^{-1}$$

A. D. Ayangeakaa *et al.*,
Phys. Rev. Lett. 110, 172504 (2013)

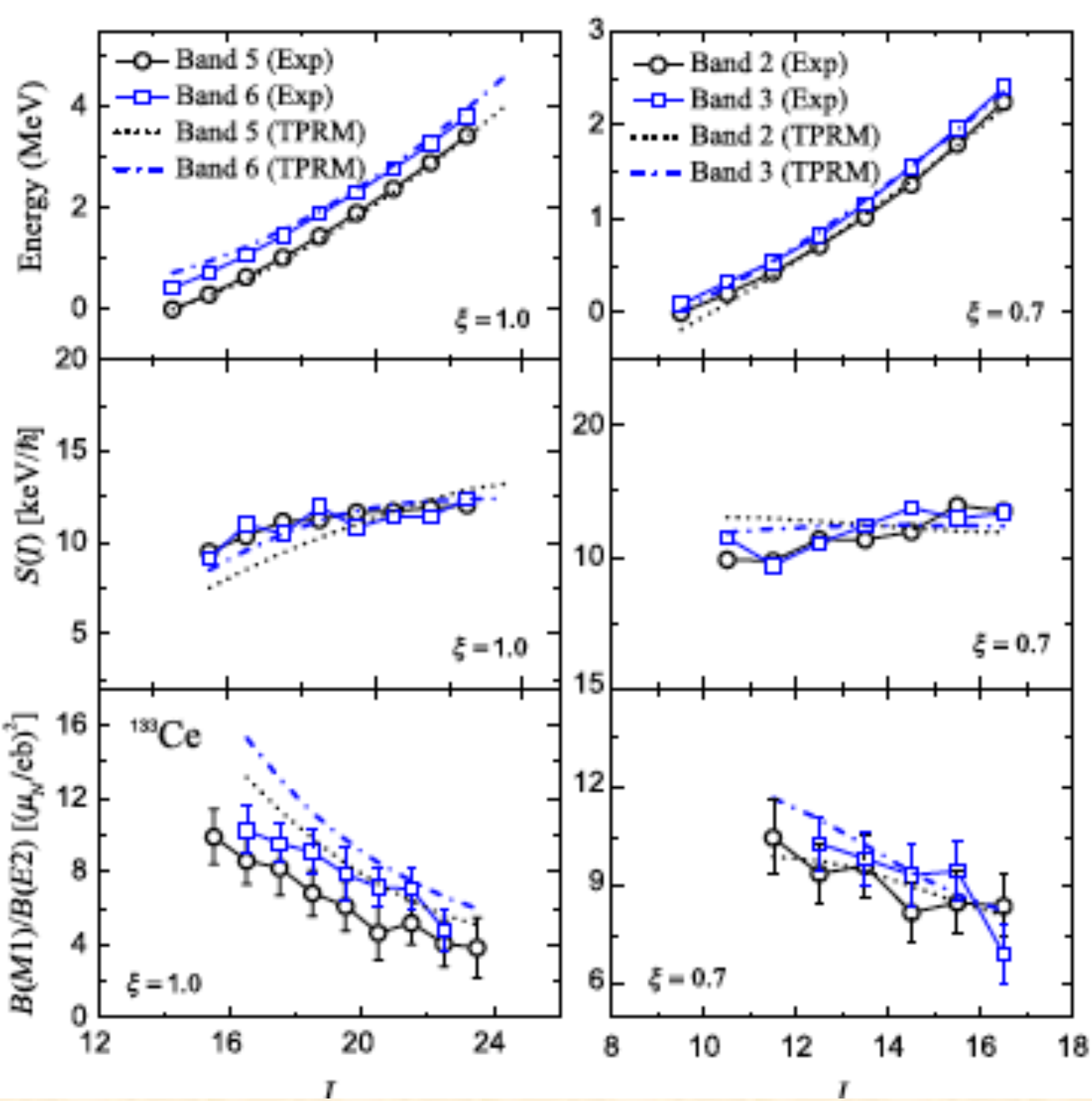

A. D. Ayangeakaa *et al.*,
Phys. Rev. Lett. 110, 172504 (2013)

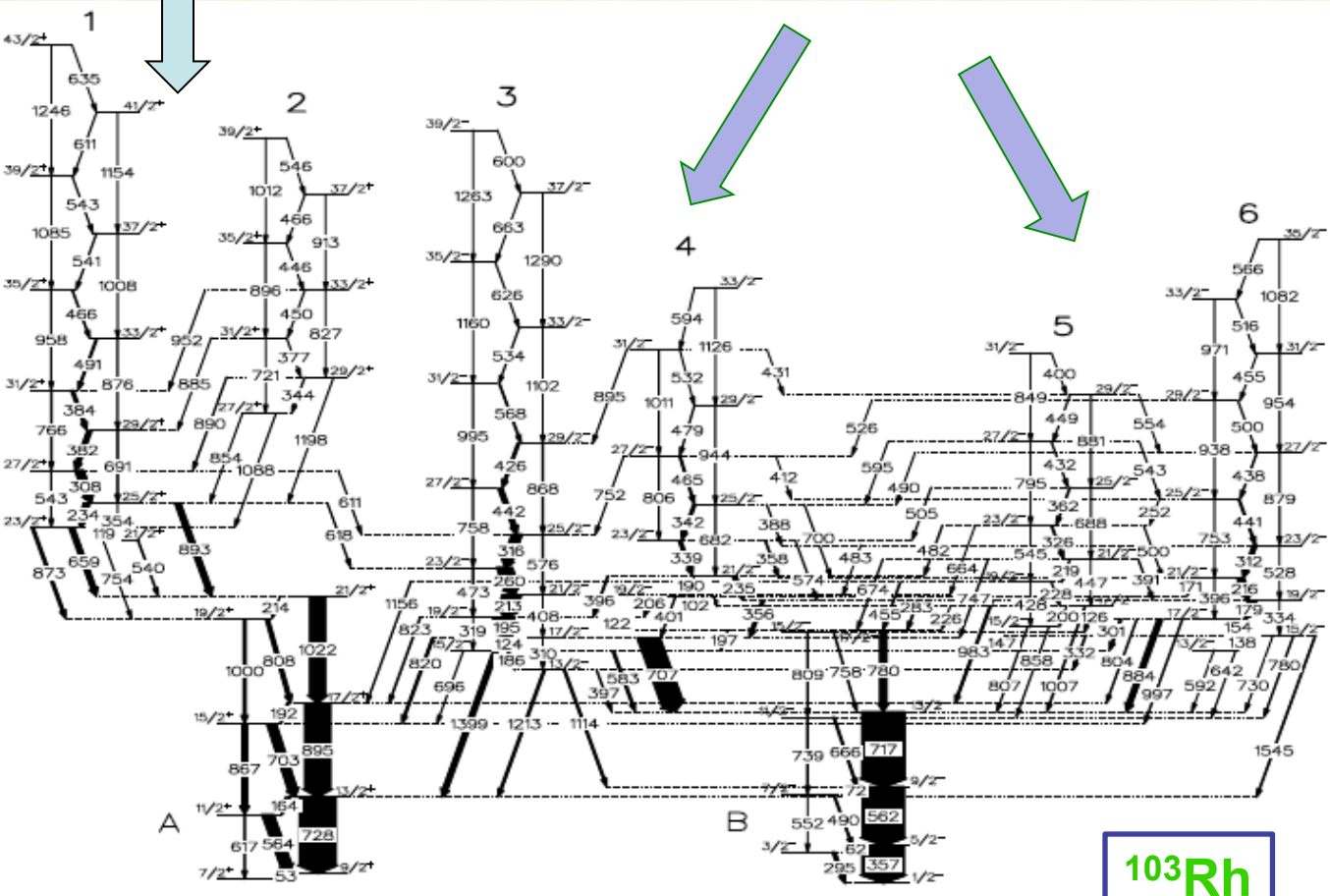

$$\pi(1g_{9/2})^{-1}\otimes\nu(1h_{11/2})^{2}$$

$$\pi(1g_{9/2})^{-1}\otimes\nu(1h_{11/2})^{2}$$

I. Kuti *et al.*, Phys. Rev. Lett. 113, 032501 (2014)

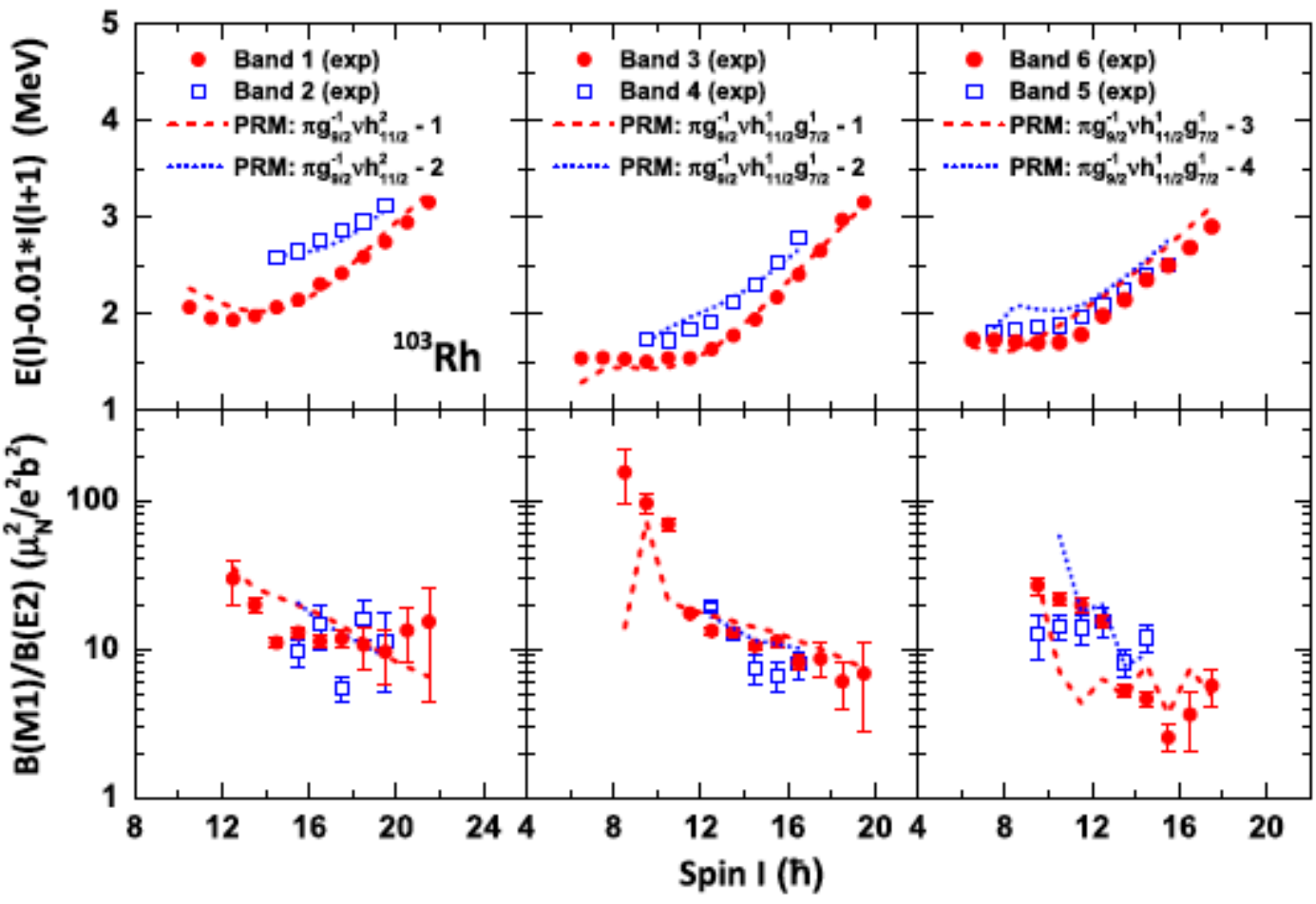

In contrast with the multiple chiral doublets predicted in Ref. [22] and experimentally reported in ^{133}Ce [26], the observed MχD in the negative-parity bands of ^{103}Rh is built from the first and second doublets of the same configuration. Although the two doublets belong to the same configuration, the angular momenta couplings for the two pairs of chiral partners are different. This fact is reflected by the different

I. Kuti *et al.*, Phys. Rev. Lett. 113, 032501 (2014)

Physics Letters B 773 (2017) 1–5

Contents lists available at ScienceDirect

Physics Letters B

www.elsevier.com/locate/physletb

Multiple chirality in nuclear rotation: A microscopic view

P.W. Zhao

Physics Division, Argonne National Laboratory, Argonne, IL 60439, USA

ARTICLE INFO

Article history:
Received 7 July 2017
Received in revised form 27 July 2017
Accepted 1 August 2017
Available online 7 August 2017
Editor: W. Haxton

Keywords:
Covariant density functional theory
Chiral rotation
Tilted axis cranking
Nuclear spectroscopy

ABSTRACT

Covariant density functional theory and three-dimensional tilted axis cranking are used to investigate multiple chirality in nuclear rotation for the first time in a fully self-consistent and microscopic way. Two distinct sets of chiral solutions with negative and positive parities, respectively, are found in the nucleus ^{106}Rh. The negative-parity solutions reproduce well the corresponding experimental spectrum as well as the $B(M1)/B(E2)$ ratios of the transition strengths. This indicates that a predicted positive-parity chiral band should also exist. Therefore, it provides a further strong hint that multiple chirality is realized in nuclei.

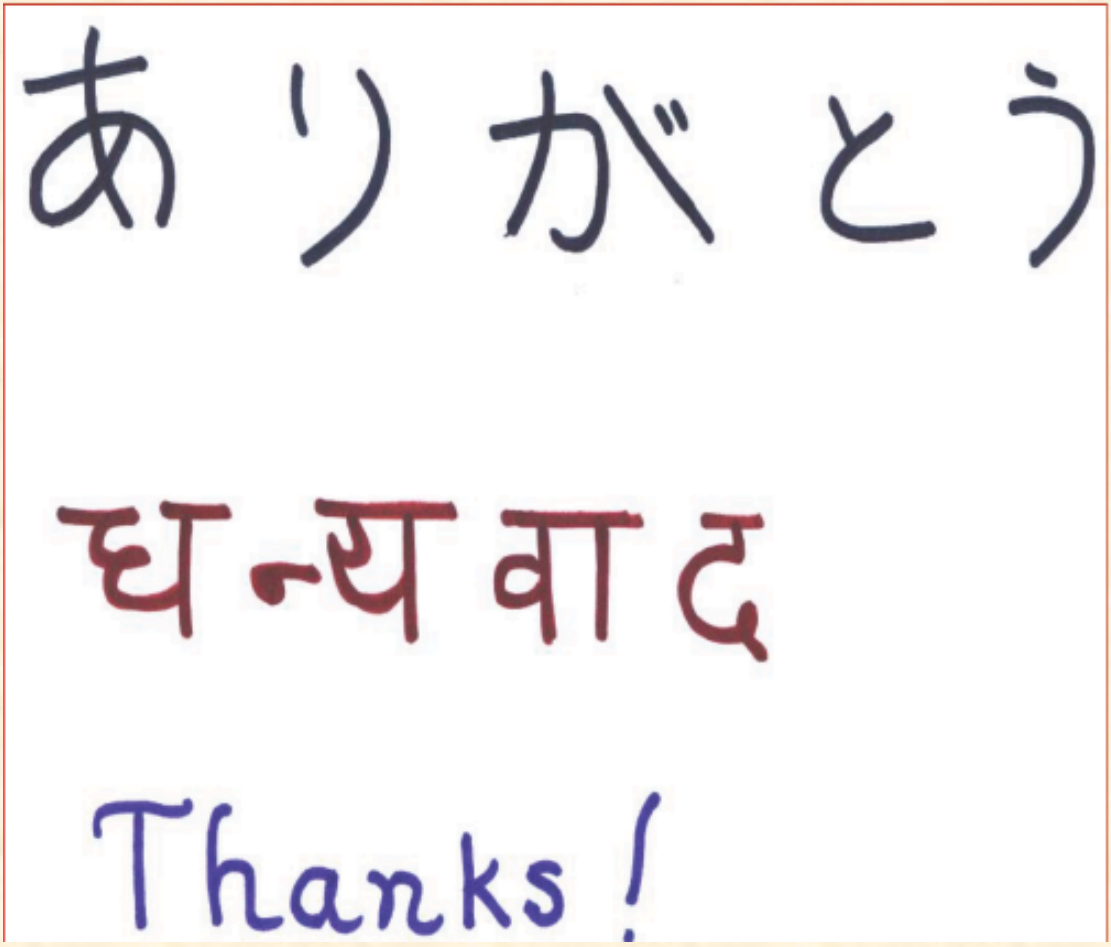
ありがとう
धन्यवाद
Thanks!

The Question Kitten